



Dyke to sill deflection in the shallow heterogeneous crust during glacier retreat: part II

Kyriaki Drymoni^{1,2} · Alessandro Tibaldi^{1,3} · Fabio Luca Bonali^{1,3} · Federico Pasquarè Mariotto⁴

Received: 5 June 2023 / Accepted: 13 March 2024 / Published online: 5 April 2024
© The Author(s) 2024

Abstract

Changes from dyke to sill propagation in the shallow crust are often caused by dissimilar layer properties. However, most previous studies have not considered the influence of glacial loading and unloading on dyke and sill deflection processes. Here, we attempt to collectively explore mechanical (layer stiffness) and geometrical (dyke dip, layer thickness) realistic parameters subject to two different magma overpressure values (namely 5 MPa and 10 MPa) that promote dyke-sill transitions in both non-glacial and glacial settings. To do this, we use as a field example, the Stardalur laccolith: a multiple stacked-sill intrusion located in SW Iceland. The laccolith lies near the retreating Langjökull glacier and was emplaced at the contact between a stiff lava layer and a soft hyaloclastite layer. We initially model two different stratigraphic crustal segments (stratigraphy a and b) and perform sensitivity analyses to investigate the likely contact opening due to the Cook-Gordon debonding and delamination mechanism under different loading conditions: magma overpressure, regional horizontal extension, glacial vertical load and a thin elastic layer at the stratigraphic contact. Our results show that contact opening (delamination) occurs in both non-glacial and glacial settings when the dissimilar mechanical contact is weak (low shear and tensile stress, zero tensile strength). In non-glacial settings, stiff layers (e.g., lavas) concentrate more tensile stress than soft layers (e.g., hyaloclastites/breccia) but accommodate less total (x - y) displacement than the surrounding host rock (e.g., soft hyaloclastites) in the vicinity of a dyke tip. Yet, a thicker hyaloclastite layer in the stratigraphy, subject to higher magma overpressure ($P_0 = 10$ MPa), may encourage dyke-sill transitions. Instead, in glacial domains, the stress conditions imposed by the variable vertical pressure of the ice cap result in higher tensile stress accumulation and displacement in stiff layers which they primarily control sill emplacement.

Keywords Sill emplacement · Glacier retreat · Iceland · FEM numerical modelling · Dyke · Inclined sheet

Introduction

Dyke propagation is associated with magma transport from the source to the surface (Anderson 1951; Pollard 1987; Rubin 1995; Menand and Tait 2002; Gudmundsson 2011a, 2020; Tibaldi 2015; Acocella 2021). This is often the case when the maximum principal compressive stress, σ_1 , is vertical, which favours the vertical propagation of magma, and occurs in geologic settings such as slow-spreading rifts (Macdonald 1982; Forslund and Gudmundsson 1991; Gudmundsson 2011b; Pedicini et al. 2023). Still, under specific mechanical conditions, magma can stall in the heterogeneous and anisotropic crust, forming intrusive bodies such as sills, laccoliths and plutons (Jaeger 1959; Pollard and Johnson 1973; Petford et al. 2000; Acocella 2000). Magma intrusions have been extensively studied so far based on their surficial deformation fingerprints (Pollard 1973; Pollard and

Editorial responsibility: J. Ruch

✉ Kyriaki Drymoni
kyriaki.drymoni@min.uni-muenchen.de

¹ Department of Earth and Environmental Sciences, University of Milan-Bicocca, 20126 Milan, Italy

² Earth and Environmental Sciences, Ludwig-Maximilians-Universität in Munich, Theresienstr.41, 80333 Munich, Germany

³ CRUST-Interuniversity Center for 3D Seismotectonics With Territorial Applications, 66100 Chieti Scalo, Italy

⁴ Department of Human and Innovation Sciences, Insubria University, Como, Italy

Holzhausen 1979; Fialko et al. 2001); however, the mechanics of their emplacement are still unclear.

Sills are bedding-parallel extension fractures (planar sheet intrusions) filled by magma (Gilbert 1877). They can be distinguished from lava flows in the field based on their well-developed columnar joints, roof and bottom chilled selvages (glassy margins) formed at the contact with the host rock and their low vesicularity (Gudmundsson 2011a, 2020; Barnett and Gudmundsson 2014; Tibaldi 2015; Acocella 2021). Their emplacement in brittle crustal segments was initially explained by the neutral buoyancy rule (Francis 1982; Corry 1988), which suggests that when an extension fracture (e.g., a dyke) crosscuts a dissimilar contact and meets a layer with the same density, it deflects along the contact forming a sill. However, field observations (Gudmundsson 1995; 2012; Burchardt 2008; Browning and Gudmundsson 2015; Drymoni et al. 2020; 2022; 2023a; 2023b), 3D seismic analyses (Thomson and Hutton 2004; Hansen et al. 2004; Hansen and Cartright 2006; Thomson 2007; Galerne et al. 2008; Magee et al. 2013), analogue experiments (Kavanagh et al. 2006; Menand 2008) and analytical models (Maccaferri et al. 2010, 2011) have shown that dykes can penetrate host rock layers and feed eruptions, even if their magma has a similar density to the country rock. Hence, we must investigate other causes for dyke-sill transitions, such as stress controls (Gudmundsson 1990; Watanabe et al. 1999; Pinel and Jaupart 2000, 2004; Valentine and Krogh 2006; Menand et al. 2010; Mathieu et al. 2015; Walker et al. 2017; Stephens et al. 2018; Walker and Gill 2020; Greiner et al. 2023), pore fluid pressure (Gressier et al. 2010), rheology contrast between ductile and brittle layers (Parsons et al. 1992; Thomson and Schofield 2008; Galland et al. 2019), rigidity contrast of the contacts (Rivalta et al. 2005; Kavanagh et al. 2006; 2015), lithological discontinuities (Gretener 1969; Barnett and Gudmundsson 2014), or stress rotation around pre-existing fractures (Drymoni 2020; Drymoni et al. 2021). Coupled methodologies, such as pairing geological observations with numerical modelling provide a better understanding of sill formation, showing their mechanical evolution into magma chambers (Hardee 1982; Coleman et al. 2004; Barnett and Gudmundsson 2014), and their thermal evolution in the layered crust (Cashman et al. 2017; Annen et al. 2006).

This is a compound article (Part II) with our previous work (Drymoni et al. 2023c) which aim to collectively explore, using finite element method (FEM) numerical modelling, the mechanical and geometrical conditions that dictate the emplacement of sills in the shallow crust in non-glacial and glacial settings. In Part I, we explored how the magma overpressure, the local stress field (extension or compression), the presence (or not) of a very weak contact influence dyke to sill deflection. We also modelled unloading scenarios subject to glacier thickness variations. Our Part

II delves into the Cook-Gordon debonding and delamination mechanism. In the first part, we modelled realistic dyke-sill transitions and attempted to simulate mechanically the scattered flower structure geometry of the Stordalur laccolith (Tibaldi and Pasquaré 2008). Specifically, we identified the conditions that influence the relative distance between the dyke and the opening contact, i.e., how close to the contact the sill was going to be emplaced. We designed a series of sensitivity tests to investigate the range of dyke pathways under realistic geologic conditions. In detail, we explored in non-glacial settings how different layered sequences (deeper or shallower crustal segments), layer stiffness and thickness, and dyke inclination encouraged or discouraged the formation of a sill closer to a mechanically weak contact. Finally, we modelled how glacier retreat, using glacier width variations, controls dyke-sill transitions in glacial settings. We answer the following questions: (1) Which mechanism controlled the emplacement of the Stordalur laccolith? (2) How do different realistic geometrical and mechanical parameters collectively affect the opening of a dissimilar contact in non-glacial and glacial settings? and (3) How do dyke-sill transitions respond to glacial settings with variable glacier widths? Our overall results aim to provide valuable insights on dyke-sill deflection processes in non-glacial and glacial settings around the world.

Sill emplacement in composite volcanoes

Sills in composite volcanoes are formed by dykes which have originally stalled along dissimilar contacts due to the heterogeneity and anisotropy of the shallow crust (Gudmundsson 2011a). Mechanically, they propagate perpendicular to the minimum principal compressive stress (σ_3) when the horizontal compressive stress is vertical (Anderson 1951; Roberts 1971; Gudmundsson 2011b) despite the presence of layered rocks. This can effectively take place at divergent plate boundaries where rapid dyke propagation (high P_o) occurs in stratified layers (Parsons et al. 1992).

Analytical models on physical failure conditions subject to static loads (He and Hutchinson 1989; Hutchinson and Suo 1992; Hutchinson 1996; Roham et al. 2004), along with field observations (Gudmundsson 2011a), have shown that when a dyke meets a contact, it may follow three possible pathways based on its mechanical interaction with the heterogeneous host rock, namely, (1) the dyke stalls at the contact (Fig. 1a), (2) the dyke deflects (kinks) or opens symmetrically or asymmetrically along a contact or a pre-existing fracture (Fig. 1b, c) and (3) the dyke crosscuts the contact and propagates through the layered succession (Fig. 1d). A sill can be formed at the first three cases (Gudmundsson and Lötveit 2012). The aforementioned dyke pathways depend on the energy release ratios of the final outcome (propagation/deflection)

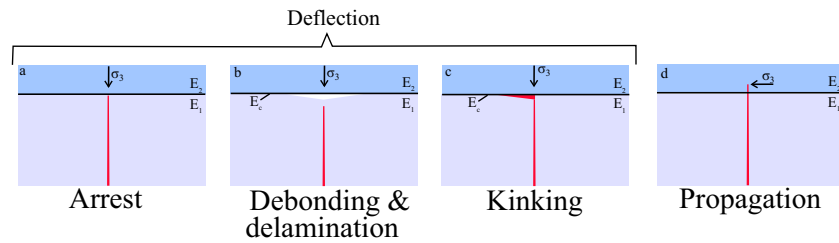


Fig. 1 Dyke (magma-filled fracture) pathways in a layered domain. **a** Dyke arrest, **b** interface debonding ahead of a dyke tip, **c** kinking or deflection of a dyke at a mechanically dissimilar contact and **d** dyke

propagation. E_1 : Young’s modulus of the bottom layer, E_2 : Young’s modulus of the top layer, E_c : Young’s modulus of the contact

and the interfacial deflected cracks, the fracture toughness (K_C) between the material of the host rock and the interface (contact) (Evans and Zok 1994; Wang and Xu 2006), the host rock geology and magma dynamics (Schofield et al. 2012).

In a general notation, if a dyke intersects a stiff (top)/soft (bottom) layered contact, dyke deflection or arrest is more common. On the contrary, if a dyke crosses a soft (top)/stiff (bottom) layered contact, then dyke propagation is almost possible (Kavanagh et al. 2006, 2018; Gudmundsson 2020; Forbes Inskip et al. 2020; Drymoni et al. 2020). This is mainly associated with the mechanical properties of the host rock and the mechanisms that control the pathway of the dyke. Hence, sill formation can occur via three mechanical concepts, which can act simultaneously or not: (1) stress barriers, (2) elastic mismatch and (3) Cook-Gordon debonding and delamination as explained below.

Mechanical concepts of sill formation and lateral propagation

Stress barriers

A temporary stress barrier is a mechanical condition encouraged by the dissimilar properties of the host rock (Gudmundsson 2020). Specifically, the contrasting stiffness (i.e., Young’s modulus) between the upper and the bottom layer of a contact where $E_{upper} > E_{bottom}$ can rotate the stress field ahead of the dyke tip (σ_1 becomes horizontal) and a dyke can be stalled. In rift zones, previous dyke injections or graben subsidence induce compressional regimes that make stiff (high Young’s modulus) layers (e.g., lava deposits) temporary stress barriers (Gudmundsson 1995; Roman et al. 2004; Geshi et al. 2012; Kusumoto et al. 2013; Tibaldi et al. 2022; Drymoni et al. 2023c). Similarly, soft (low Young’s modulus) layers, such as pyroclastic deposits, tend to concentrate the horizontal compressive stress especially in areas under local extension (Gudmundsson and Brenner 2001) and become stress barriers as well. Stress barriers can generate asymmetric sills (after the initial arrest) if the overpressure of the dyke (P_o) overcomes the tensile strength (T_o) of the

contact and its vertical stress (which is equal to σ_3 in arrested contacts), so as to lift the overburden (Gudmundsson 2012). Yet, similar stress rotations can effectively produce from stress effects of previous dyke intrusions that carry overpressure ‘residual’ stresses. The latter encourage locally horizontal compression, which is finally restored through plate movements (Gudmundsson 2020).

Elastic mismatch

Elastic mismatch is a mechanism associated with the mechanical properties of the contact (i.e., Young’s modulus) and particularly the critical elastic strain energy or material toughness (G_{IC}) of the adjacent layers. It usually occurs in composite materials (He and Hutchinson 1989; Freund and Suresh 2003), and it is mechanically described as an energy concept in mixed fracture modes (Sun and Jin 2012). It usually encourages dyke-arrest concepts when the elastic mismatch between two adjustment layers increases (García 2014). However, this mechanism can promote dyke-arrest scenarios or dyke-sill transitions equally if operating collectively with other mechanisms such as the Cook-Gordon debonding and delamination mechanism (Gudmundsson 2020; Clunes et al. 2021). In the second case, the dyke propagates as a mixed mode fracture; hence, the deflection condition is expressed from Eq. (1) (Gudmundsson 2011a):

$$\frac{G_d}{G_p} \geq \frac{\Gamma_{D(\Psi)}}{\Gamma_L^1} \tag{1}$$

where G_d is the energy release rate for deflection and G_p is the energy release rate for propagation at the contact; Γ_D is the critical elastic strain energy or material toughness at the contact (or discontinuity) and is the material toughness above the layer. Ψ is the relative proportion of the fracture modes in each case study (e.g., mode I and mode II fracture), which is associated with the critical stress intensity factor (or material toughness) K_c .

However, the relative energy release rate (G_d) relates to the mechanical properties of the discontinuities and

especially the Dundurs elastic mismatch parameter (α) (Dundurs 1969). Analytical (He et al. 1994) models and analogue (Kavanagh et al. 2017) and natural-material experiments (Forbes Inskip et al. 2020) show that when the stiffness ratio of the contact equals 1 and the Dundurs parameter α equals 0, then dyke-sill deflection occurs only if the material toughness of the contact is 26% less than that of the layer above (Gudmundsson 2011a; Barnett and Gudmundsson 2014). Further experimental (Kim et al. 2006) and analogue studies (Kavanagh et al. 2006) have also explored deflection conditions since they are usually found at contacts between a stiff (top)/soft (bottom) layer.

Cook-Gordon debonding and delamination

The Cook-Gordon debonding and delamination mechanism is often identified in engineering concepts of composite materials (Cook and Gordon 1964; Gordon 1976; Gupta et al. 1992; Martinez and Gupta 1994; Lee et al. 1996; Majumdar et al. 1998; Leguillon et al. 2001; Barber et al. 2002). Dynamic crack-propagation experiments in layered (Xu and Rosakis 2003) and viscoelastic materials (Gori et al. 2018) or biomaterial interfaces (Rosakis et al. 1998) have shown that apart from dynamic intralayer or interfacial failure criteria, crack propagation may occur without the fracture to penetrate the contact (Wang and Xu 2006). This can be satisfied when a vertical fracture (e.g., a dyke) with high tensile stress (σ_3) concentration at its tip approaches a very weak (in tension and shear) mechanically dissimilar contact (tensile strength (T_o) close to zero) (Gudmundsson 2011a). This occurs when the tensile stress that acts parallel to the dyke tip becomes almost 20% of its perpendicular expression (usually around 2–3 MPa), or the dyke overpressure increases predominantly (i.e., 20–30 MPa). Those conditions occasionally rupture the host rock ahead of the dyke tip and assist in fracture growth (Gudmundsson 2020). The open contact progressively transitions into a mixed mode or a shear mode (mode II) as it propagates away from the centre of the delamination due to the increasing interfacial shear stress (τ). Finally, the delamination generates mode I microcracks behind the crack tip, until the bottom layer, which is still under tension (at the horizontal level), to fragment (Rosakis et al. 2000; Xu and Rosakis 2003). This mechanism may explain the formation of sills and dyke-arrest scenarios (Gudmundsson 2003; Barnett and Gudmundsson 2014) in the shallow crust when the energy criterion (Eq. 1) cannot successfully predict the probability of crack deflection or propagation (Ahn et al. 1998; Lee et al. 2004; Wang and Xu 2006). The crack pathway is collectively controlled by the magma overpressure (P_o) and the tensile strength (T_o) of the contact. In case of deflection, the magma overpressure is higher than the sum of the tensile strength of the contact and the vertical stress (σ_3 for bedding parallel fractures).

However, if the magma overpressure cannot overcome the previous sum, dyke arrest may occur.

Sill (lateral) propagation

An important condition for the lateral propagation of a sill and the subsequent formation of a pluton (inflation) is that the system is able to acquire sufficient pressure (Pollard and Johnson 1973; Corry 1988; Cruden and Weinberg 2018). During a sill's incipient conditions, most frequently, it deforms in an elastic or elastic–plastic manner, and the surrounding host rock deforms subject to its length-scale growth. Specifically, if the lateral extension is less than the sill's vertical thickness, the surrounding deformation follows elastic conditions. However, if the sill expands laterally, overburden bending can be observed atop the sill (Pollard and Johnson 1973; Rubin 1993). If the sill is partially molten (ductile condition), propagation in the horizontal plane occurs when the margins of the sill rupture due to lateral stretching. Therefore, the maximum extension usually creates blunt terminations. Yet, if brittle conditions arise, fractures at the margins of sills develop due to tensile splitting (Pollard and Johnson 1973).

Nowadays, field observations of sills have revealed more mechanisms of sill propagation. Some of them introduce the fluidization (Schofield et al. 2012) or the shear failure (Merle and Donnadieu 2000; Abdelmalak et al. 2012; Spacapan et al. 2017) of the host rock. In the first model, the magmatic heat can increase the pore fluid pressure in the surrounding host rock activating its fluidization through which the magma can be transported laterally (Schofield et al. 2012). In the second model, highly viscous magmas may generate shear stresses that rupture and deform the host rock (Merle and Donnadieu 2000; Abdelmalak et al. 2012; Spacapan et al. 2017). After its formation, a sill can vertically inflate and subject to roof lifting or floor depression a laccolith or a lopolith can be formed (Cruden 1998).

Magma chamber/laccolith formation

Sills are found in nature in a range of sizes and geometries (Smallwood and Maresh 2002; Tibaldi et al. 2008; Tibaldi and Pasquaré 2008; Burchardt 2008; Morgan et al. 2008; Gudmundsson and Løtveit 2012; Magee et al. 2016, 2017; Gudmundsson et al. 2018, 2020), and their emplacement has been studied through analogue experiments (Xu et al. 2003; Xu and Rosakis 2003; Rivalta et al. 2005; Galland et al. 2009) and analytical (Gudmundsson 1990; Pinel and Jaupart 2004; Bungler and Cruden 2011) and numerical (Gautneb et al. 1989; Grosfils et al. 2015; Barnett and Gudmundsson 2014; Haug et al. 2018; Walker and Gill 2020; Browning et al. 2021) modelling. Depending on their size (geometry and dimensions), degree of concordance and emplacement

rate, intrusive bodies are classified into different types (Crudden and McCaffrey 2001; Menand 2008; Galland et al. 2018). The difference between strata-concordant sills and laccoliths depends on their dissimilar width-scale growth and composition. A sill grows laterally (bedding-parallel), whereas laccoliths are usually felsic intrusions which primarily extend their vertical dimension (thickness) (Schmiedel et al. 2017). A conceptual model that interprets the formation of laccoliths (e.g., stacked sills) has been proposed by Morgan (2018). The latter follows Pascal's principle, and it is based on the Henry Mountains intrusions in Colorado Plateau. The model introduced two stages of magma emplacement. In the first place, the sill expands horizontally until its lateral propagation becomes sufficient to overcome the lithostatic pressure. When the previous conditions are met, then the intrusion begins to inflate, and stacked sills/upward expansion occurs. In a later stage, laccoliths can continue to grow, forming plutons (Fedotov 1981; Menand 2008; Galland et al. 2018).

Analytical models (Smith and Shaw 1975; Petraske et al. 1978; Fedotov 1981; Hardee 1982), field observations (Tibaldi and Pasquaré 2008), analogue experiments (Kavanagh et al. 2015) and geochronological data (Coleman et al. 2004; Glazner et al. 2004; Menand 2008; Michel et al. 2008) have shown that repetitive mafic magma intrusions that are emplaced atop or below already-formed sills, under specific conditions, can be taken as incipient conditions for the development of magma chambers. Still, the coalescence of smaller, nearby liquid-phase sills to develop into a magma chamber has also been proposed as an option (Gudmundsson 2011b). For that to occur, the rate of dyke injection should be high (as it commonly happens in rift zones) and the time needed for a sill to solidify must be long, implying originally thicker sill intrusions (Annen 2009).

The Stardalur laccolith-geological constraints

The Stardalur laccolith is located nearby the Langjökull glacier (approximately 25 km × 50 km in size) in the Esja peninsula proximal to the western volcanic rift zone. The laccolith's structural analysis has been reviewed by previous studies (Fridleifsson 1977; Pasquaré and Tibaldi 2007; Tibaldi and Pasquaré 2008; Drymoni et al. 2023c). Briefly, the geology of the research area is composed of basaltic lavas, hyaloclastites, volcano/sedimentary breccias and fluvial deposits (Plio-Pleistocene), cut by several magmatic intrusions and covered by lavas younger than 0.8 Ma old. The magmatic intrusions include dykes, inclined sheets and a major intrusive body, a multiple-sill laccolith, nested within a swarm of centrally dipping sheets. The laccolith is emplaced at the dissimilar mechanical contact between stiff lavas (top) and soft hyaloclastites/breccias (bottom) (Fig. 2). Further field implications can be found in Part I (Drymoni et al. 2023c).

FEM numerical modelling

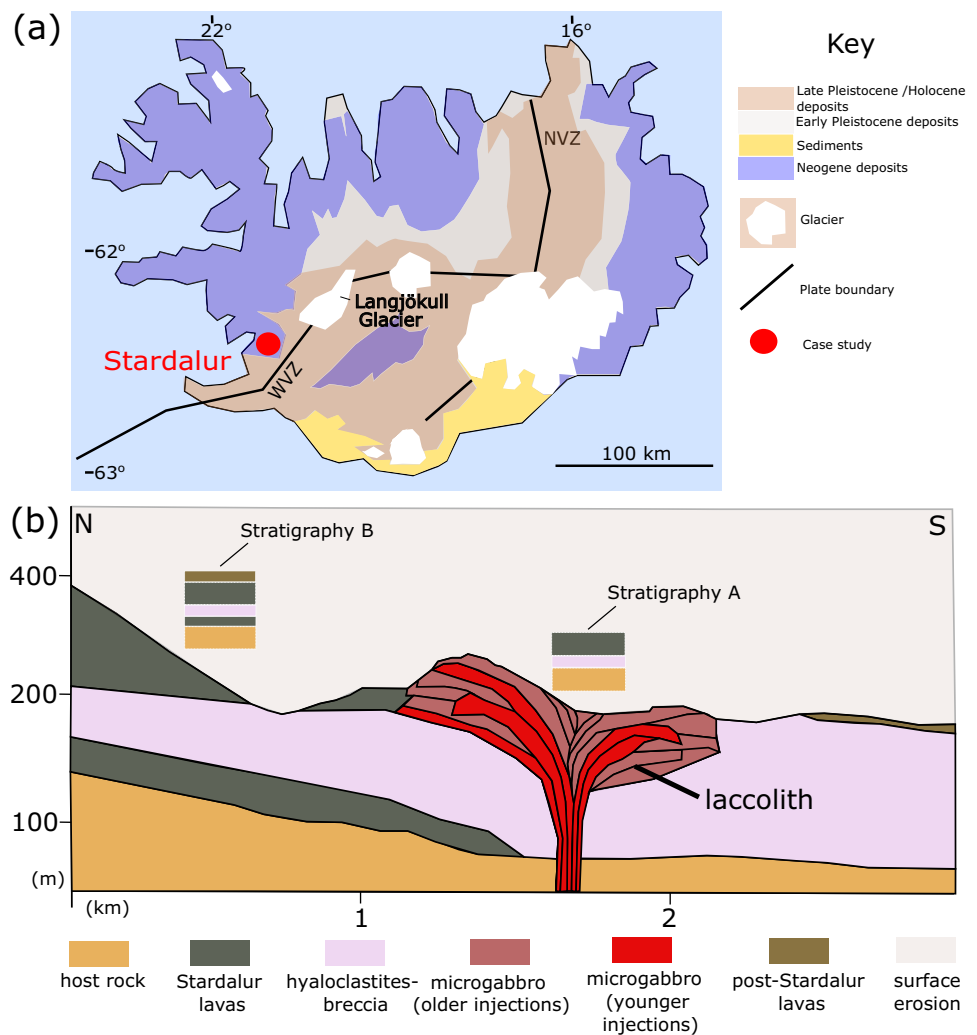
To unravel the volcanotectonic processes responsible for the formation of the Stardalur's stacked-sill structure, we used an FEM numerical method and especially the software COMSOL Multiphysics® (v6.1) (www.comsol.com). The structural mechanics module allowed us to investigate dyke to sill deflection in the shallow elastic crust and explore the displacements, stresses and strains in a solid mechanics' interface. We designed linear elastic (isotropic) material models and defined distinct material properties for the host rock layers. Since our study focused on dyke propagation and specifically the deflection at a mechanical dissimilar contact, we developed a steady-state analysis. In our models, we hypothesize that subject to sufficient fluid pressure, the magma can debond and delaminate (open) a weak (soft) contact and then propagate at the open contact between dissimilar layers. This refers to the conditions of failure in a composite material (García 2014) which leads to the separation of its layers at a contact and may act as a proxy and satisfy the mechanical concept of dyke-sill transition in the shallow crust.

Physics-based model setups and material properties

We designed two-dimensional plane strain physics-based models based on three conceptual settings (Fig. 3a–c) to simulate dyke-sill transitions in non-glacial and glacial regimes. Although three-dimensional models contain more realism and can greatly account for depth, they are computationally expensive (Depree et al. 2010). Since our studied process relies on boundary conditions that do not alter in one dimension, the use of 2D analysis is preferred as a matter of simplification. The first two non-glacial settings (Fig. 3a, b) were accommodated in a 1500 m × 1400 m rectangle domain to replicate dyke-sill deflection in the mesoscale (m to several km). The third setting was hosted in a 25 km × 25 km box domain since we wanted to explore how glacier retreat, using glacier width variations, controls dyke-sill transitions in glacial settings (Fig. 3c).

For the non-glacial setting, we fastened only the bottom corners of the model setups to avoid rotation. For the glacial setting instead, we applied fixed constraint conditions by fastening both the bottom and top corners as well as the two margins of the glacier to allow it to deform (and the contact to open) without the glacier to dislocate or slip from the free top surface. For all our models, we designed the dykes further away from the margins to avoid translation and side effects (Browning et al. 2021) and exaggerated the top and bottom layers to allow the dyke to move in the vertical axis. Finally, we performed a fine

Fig. 2 **a** Geological map of Iceland modified from Árnadóttir et al. (2023) indicating the location of the main plate boundaries and volcanic zones, the current size of the glaciers and the Stardalur laccolith. **b** Schematic illustration of the crustal segment in which the Stardalur laccolith is emplaced, modified from Tibaldi and Pasquaré (2008). Highlighted are the different stratigraphic segments (stratigraphy A and B) based on which the numerical models have been designed. WVZ, western volcanic zone; NVZ, northern volcanic zone



triangular user-defined, extremely fine mesh with a maximum element size of 15 m and a minimum element size of 0.03 m, respectively.

To study the non-glacial setting, we designed two-layered domains based on our field observations (Fig. 2b). Previous studies (Tibaldi and Pasquaré 2008) allowed us to investigate how the complex, local, heterogeneous and anisotropic crustal segment could encourage or discourage the formation of the Stardalur laccolith. In specific, our main aim was to examine whether the laccolith could have been equally emplaced in both localities (a and b) if the deflected dykes could have followed different pathways. Our secondary aim was to understand if the emplacement of the laccolith was mainly controlled by the mechanical properties of the layers (e.g., stiffness of the hyaloclastite), the overpressure (P_o) of the dyke, or if other geometrical parameters could have influenced the opening of the contact (e.g., thickness of the hyaloclastite, dip of the dyke) in the same degree.

We assigned a range of stiffness (Young's modulus) values for the different stratigraphic units based on literature

data (Gudmundsson 2011a). In specific, for the deeper geological units which serve as basement lithologies, we used $E_h = 30$ GPa, and for the Stardalur and post-Stardalur lavas, we used $E_l = 10$ GPa. To examine the effect of a soft or a comparatively stiff layer, we used two different orders of magnitude for the hyaloclastite/breccia deposits, namely $E_h = 0.5$ GPa and 5 GPa, respectively. We modelled a very soft 10-m-thick (d_s) lava_(top)/hyaloclastite_(bottom) contact with stiffness (E_c) equal to 0.001 GPa, density equal to $\rho = 2000$ kg m⁻³, Poisson's ratio (ν) equal to 0.25, and mesh element (lne) equal to 2 using the thin elastic layer node. Based on the bibliography, the term 'soft' refers to an elastic contact with low Young's modulus (stiffness) (Shull 2002) while the term 'weak' refers to the mechanical properties of the contact (low fracture resistance or fracture toughness response) (Rosakis 2002).

We performed sensitivity tests and explored the effect of the dip of the dyke and the thickness of the hyaloclastite on dyke-sill deflection. Particularly, we altered the geometry of the dyke and modelled namely a vertical (90°) dyke and an

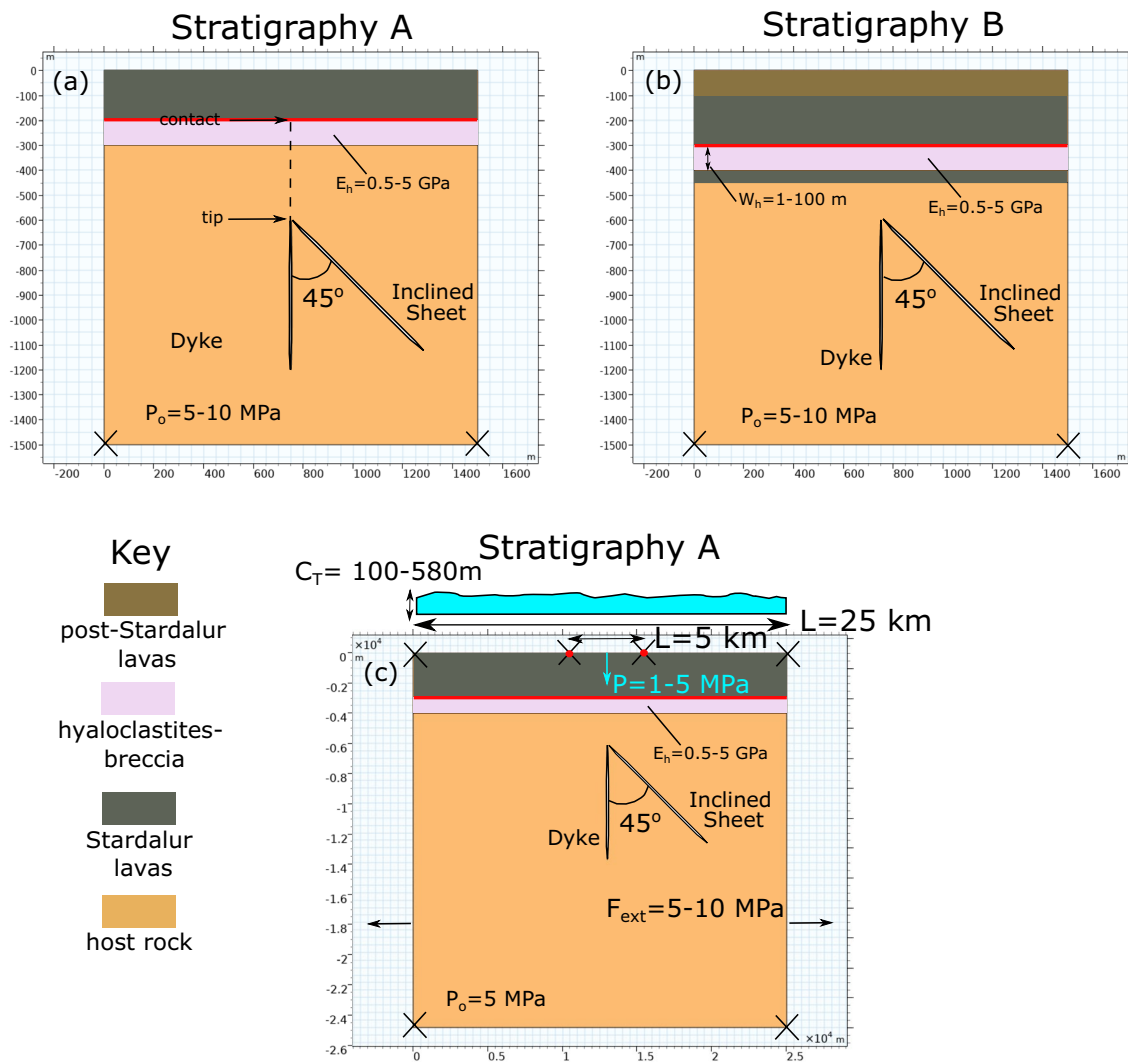


Fig. 3 Model setups for the two different stratigraphic sections (a) and (b) (shown in Fig. 2) and the glacial domain (c). The red line denotes the soft contact

inclined (45°) sheet. In addition, we changed the thickness of the hyaloclastite, and we modelled three different orders of magnitude namely 1 m, 10 m and 100 m based on our field observations (Fig. 2). In the analysis, although pre-existing fractures (faults and dykes) can be found in the shallow crust and have been shown to influence the paths of propagating sheet intrusions (Greiner et al. 2023), here, we do not account for dyke-fault interactions (Drymoni et al. 2021) or their effects (Corti et al. 2023) in dyke-sill transition. Also, we do not account for the debonding of the contact since the latter refers to the conditions that allow the physical, chemical, or mechanical forces that hold the bonds together to break (Rosakis 2002; Srinivasan and Idapalapati 2021).

For the glacial scenario, we modelled dyke-sill transition concepts for two different glacier widths equal to 25 km and 5 km, respectively. We modelled a glacier thickness (C_T)

equal to 580 m for a 25-km-wide glacier which represents the current size of the nearby Langjökull glacier (Björns-son et al. 2006). Also, we modelled a glacier thickness (C_T) equal to 100 m to mimic a future scenario where the same glacier will be 5 km wide. For all the glacial models, we used the simplest stratigraphic setting, represented by stratigraphy A in Fig. 2b.

We imported a 1-m-thick dyke at the centre of the first two non-glacial settings, and a 5-m-thick dyke at the glacial setting. We modelled the dykes as cavities without internal material properties. Based on analytical solutions (Drymoni et al. 2020) if the stiffness of the crust is 5 GPa, then a 5 MPa dyke overpressure refers to a 1.68-m-thick dyke and a 10 MPa dyke overpressure refers to a 2.32-m-thick dyke, respectively. Here, the different thickness of the cavities served only its graphic representation in the models; instead,

the magma overpressure at their boundaries was equal to 5 MPa and 10 MPa, respectively. Finally, the depth of the stratigraphy was designed based on the schematic illustration in Fig. 2b, and the location of the dykes was set arbitrarily at the centre of the domain.

We performed a sensitivity analysis to explore the maximum distance of the dyke tip required to open a dissimilar mechanical contact by trial and error via the following steps: (1) we designed several ‘reconnaissance’ models in which we gradually changed the location (static model snapshots) of the dyke tip (in Y -axis) closer to the dissimilar mechanical contact. In every model, we recorded the total (x - y) displacement values until we finally obtained the highest calculated value which was recorded when the dyke tip-contact distance was almost zero; (2) we reran the models, as explained before, and obtained the location of the dyke tip (distance from the contact and/or depth of the dyke tip) where the contact opened; and (3) we used the same methodology for all the final model comparisons.

Numerical analysis

We designed four boundary loading conditions to replicate the physical processes which encourage or discourage the delamination (opening) of the soft contact in a non-glacial and glacial setting. The conditions were gradually built up in the models and were namely (a) a magma overpressure load (P_o) performed as a pressure load at the boundaries of the dyke cavity, to simulate the internal, net pressure of the dyke; (b) a thin elastic layer performed as a boundary load at the lava/hyaloclastite contact, to mimic a very soft contact capable to delaminate; (c) a vertical boundary load, applied as a pressure load, to replicate the glacier’s imposed

weight (compressional setting) at the top free surface; and (d) a horizontal boundary load, performed as a pressure load perpendicular to the Y -axis domain margins, to represent the extensional regime induced by glacier rebound. The thin elastic layer acted as a boundary load, which had a very low Young’s modulus value (E). The steady-state study is explained in detail in Part I (Drymoni et al. 2023c).

We assigned a constant magma overpressure equal to $P_o = 5$ MPa to all our models, but for the sensitivity analyses where we explored the effects of magma overpressure on dyke-sill deflection, we modelled two different values, namely 5 MPa and 10 MPa. The selected values could generate the minimum amount of tensile stress (σ_3) needed to open the contact (Gudmundsson 2020). We applied a vertical pressure boundary load equal to $P = 5$ MPa to model the vertical load of the glacier. Finally, we applied a horizontal extension (F_{ext}) equal to 5 MPa at the vertical margins of the domains to model the extensional regime induced by glacier rebound (Stewart et al. 2010).

We designed a tensile stress surface (in MPa), which showed the accumulation of tensile stress (σ_3) around the dyke tip and at its vicinity. We modelled two arrow surfaces, which showed the orientation of two of the principal compressive stresses (σ_1 and σ_2), hence the magma propagation pathway (which is parallel to σ_1), ahead of the dyke tip. In addition, we designed a total x - y displacement surface (in km due to the glacier size) that allowed us to observe the scenario of contact opening (or not) in each model. The opening of the contact was visible as a white area, which subject to higher magma overpressure values or the dyke tip-contact distance became thicker at the centre above the dyke tip and faded away at its margins. All the models and modelling parameters are summarised in Table 1.

Table 1 A summary of all the different models presented in this study. Bold entries represent tensile stress and displacement surfaces while the italic entries represent displacement surfaces

Models	
Boundary loads and studied parameters	Stratigraphy A
	Stratigraphy B
	<p>No ice cap</p> <ol style="list-style-type: none"> $E_{hyaloclastite}$ v_S tip-contact distance for a given dyke overpressure ($P_o = 5$ MPa) (vertical dyke, inclined sheet) (Fig. 4) <i>Tip-contact distance v_S dyke overpressure ($P_o = 5$ MPa and 10 MPa) (vertical dyke) (Fig. 5)</i> <p>With ice cap</p> <ol style="list-style-type: none"> <i>An ice cap subject to width adjustments for a given dyke overpressure ($P_o = 5$ MPa) (vertical dyke, inclined sheet) in non-glacial and glacial settings (Fig. 8)</i> <ol style="list-style-type: none"> $E_{hyaloclastite}$ v_S tip-contact distance for a given dyke overpressure ($P_o = 5$ MPa) (vertical dyke, inclined sheet) (Fig. 6) <i>$W_{hyaloclastite}$ v_S $E_{hyaloclastite}$ v_S dyke overpressure ($P_o = 5$ MPa and 10 MPa) (vertical dyke) (Fig. 7)</i>

Results

Stratigraphy A

In the first suite of models, we explored how the stiffness of the hyaloclastite controlled the opening of the contact when the dyke tip-contact distance was (1) 40 m and (2) 8 m, respectively. In the first model (Fig. 4a), where the hyaloclastite was soft and the dyke tip was deeper in the domain, we observed moderate tensile stress concentration (3–6 MPa) around the dyke tip while the principal compressive stress (σ_1) remained (almost) vertical at the

vicinity of the dyke tip. The model in Fig. 4b showed moderate values (0.6 m) of displacement around the dyke, and no contact opening occurred at the soft contact ahead. In the next run, we increased the stiffness of the hyaloclastite by one order of magnitude (Fig. 4c). The tensile stress concentration increased inside the comparatively stiff layer. The arrow surfaces (σ_1 and σ_2) showed no stress rotations at the vicinity of the dyke tip. The displacement values (Fig. 4d) decreased around the dyke showing that a stiffer material could accommodate less (x - y) displacement in similar loading conditions. Yet, the soft contact did not open.

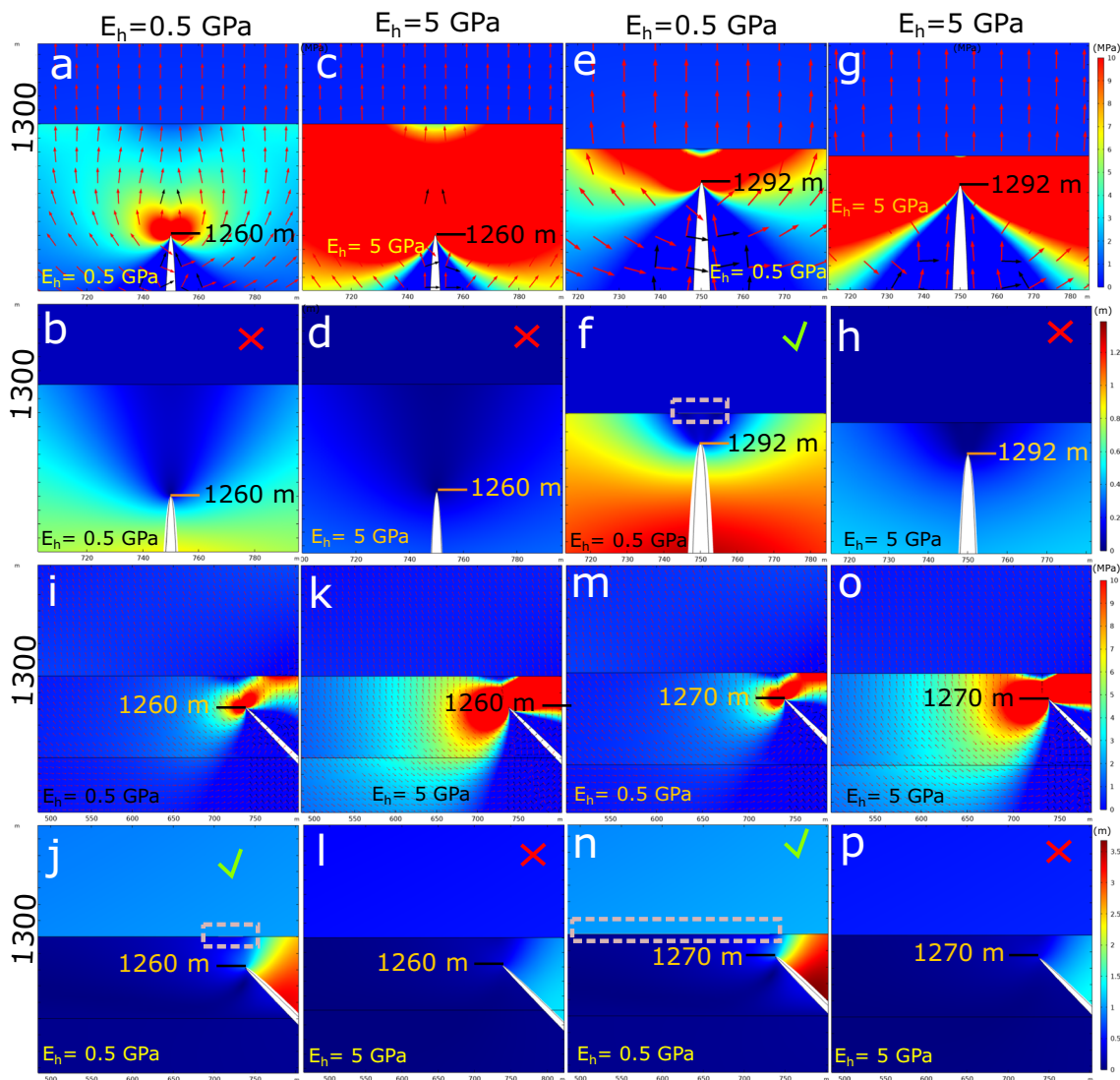


Fig. 4 COMSOL models showing the tensile stress concentration (a, c, e, g, i, k, m, o) (in MPa) and (x - y) displacement magnitude (b, d, f, h, j, l, n, p) (in m) around a dyke tip subject to dissimilar host rock mechanical properties (stratigraphy a). The magma overpressure is constant ($P_o=5$ MPa), the red arrows show σ_1 , and the black arrows

show σ_2 . The dashed boxes indicate the location and size of the contact opening. The crosses indicate no contact opening while the ticks indicate opening of the weak contact. The figure snapshots show only a part of the models

We moved the dyke tip shallower, at a depth where the contact could delaminate. When the hyaloclastite was soft (Fig. 4e), the tensile stress concentration increased ahead of the dyke tip and the σ_1 arrows rotated (around 45°). The displacement values (Fig. 4f) increased around the dyke (0.8–1.4 m), and the soft contact opened. In the next runs, we increased the stiffness of the hyaloclastite ($E_h = 5$ GPa) (Fig. 4g). Although the results were similar to the previous runs, the displacement values around the dyke decreased (0.2–0.4 m) and the contact did not open.

In the next round, we tested the effect of an inclined sheet in the same stratigraphic sequence. For the inclined sheet models, we showed larger parts of the models to fit the lateral size of contact opening. We explored how the stiffness of the hyaloclastite controlled the opening of the contact when the dyke tip-contact distance was (1) 40 m and (2) 30 m, respectively. Our models did not develop stress rotations in any of the studied concepts (Fig. 5i, k, m, o), and the tensile stress concentration was similar to the previous runs (Fig. 4j, l, n, p). The displacement models (Fig. 4j, n) showed that when the hyaloclastite was soft, the contact could open once the dyke tip was deeper in the domain (Fig. 4b). In addition, contact opening became longer in the X-axis opposite to the acute angle of the dip while the dyke tip got shallower (Fig. 4n). However, when the hyaloclastite layer became stiffer, in both studied depths (40 m and 30 m, respectively), the contact did not open (Fig. 4l, p).

Tip-contact distance vs contact delamination subject to different overpressure (P_o) values

We studied the opening of a soft lava/hyaloclastite contact induced by a dyke tip that it was located along the y - y' axis subject to different overpressure conditions. We used the simplest model setup (stratigraphy a), and we captured six models (displacement snapshots). The dyke was set in arbitrary Y -axis positions to investigate the theoretical depth of the dyke tip that could open the soft contact ahead. In the first group of models (Fig. 5a–f), the stiffness of the top lava layer was $E_l = 10$ GPa, the stiffness of the bottom hyaloclastite layer was $E_h = 0.5$ GPa, and the stiffness of the contact was $E_c = 0.0001$ GPa. The magma overpressure (P_o) was 5 MPa and remained constant during the static runs. We progressively moved the dyke closer to the soft contact and observed that it opened when the dyke tip-contact distance was 24 m. The maximum displacement around the dyke increased gradually while the dyke-tip was approaching the soft contact and reached its highest value which was equal to 1.6 m. In the next runs (Fig. 5g–l), we kept the same material properties for the dissimilar layers and the contact but increased the magma overpressure ($P_o = 10$ MPa). The models showed that the contact opened when the dyke was now deeper in the domain (tip-contact distance was 33 m).

The maximum displacement was proportional to the overpressure increase and equal to 3.2 m.

Stratigraphy b

We reran the previous model suites using the second stratigraphic setup (stratigraphy b). The soft contact was now deeper in the domain (tip-contact distance was 30 m). In the first model, where the hyaloclastite was soft (Fig. 6a), the tensile stress (4–10 MPa) was concentrated in the soft layer, and no stress rotations were observed in it. When we increased the stiffness of the hyaloclastite ($E_h = 5$ GPa) (Fig. 6c), the layer concentrated more tensile stress (9–10 MPa) than before. In both cases, the models indicated that the displacement around the dyke tip was low (up to 1.6 m) and the contact did not open (Fig. 6b, d). We moved the dyke tip closer to the contact (tip-contact distance was 20 m) (Fig. 6e, g). The tensile stress accumulation around the dyke tip was similar to the previous runs (Fig. 6a, c). However, the displacement models (Fig. 6f, h) showed that the contact could open only if the hyaloclastite was soft.

In the next round, we tested the emplacement of an inclined sheet in the domain. The tensile stress accumulation around the inclined sheet was similar to the previous runs (Fig. 5i, k). When the tip of the inclined sheet was deeper (tip-contact distance was 50 m), the contact did not open regardless of the stiffness of the hyaloclastite. Finally, we moved the tip closer to the contact (tip-contact distance was 20 m). The tensile stress accumulation was similar to the previous runs (Figs. 5m, o and 6m, o). The displacement models showed that the soft hyaloclastite layer encouraged the opening of the contact at this depth (Fig. 6n).

Layer thickness vs layer stiffness subject to different magma overpressure (P_o) values

In this set of models, we explored how the thickness and the stiffness of the hyaloclastite layer collaboratively controlled the opening of the soft contact subject to different magma overpressure values. In the first four runs (Fig. 7a, b, e, f), we modelled a very thin hyaloclastite layer ($W_h = 1$ m) with soft and comparatively stiff mechanical properties, respectively, subject to two different magma overpressure values, namely 5 MPa and 10 MPa. The results showed that the contact opened only when the layer was soft ($E_h = 0.5$ GPa) and the overpressure was high ($P_o = 10$ MPa).

In the next four runs (Fig. 7c, d, g, h), we increased the thickness of the hyaloclastite by one order of magnitude ($W_h = 10$ m). Interestingly, the results showed that the soft contact opened when the hyaloclastite was stiff, and the magma overpressure was high ($P_o = 10$ MPa). In specific, when the hyaloclastite was soft, the displacement increased around the dyke margins (1.5–2.5 m) but not around the dyke

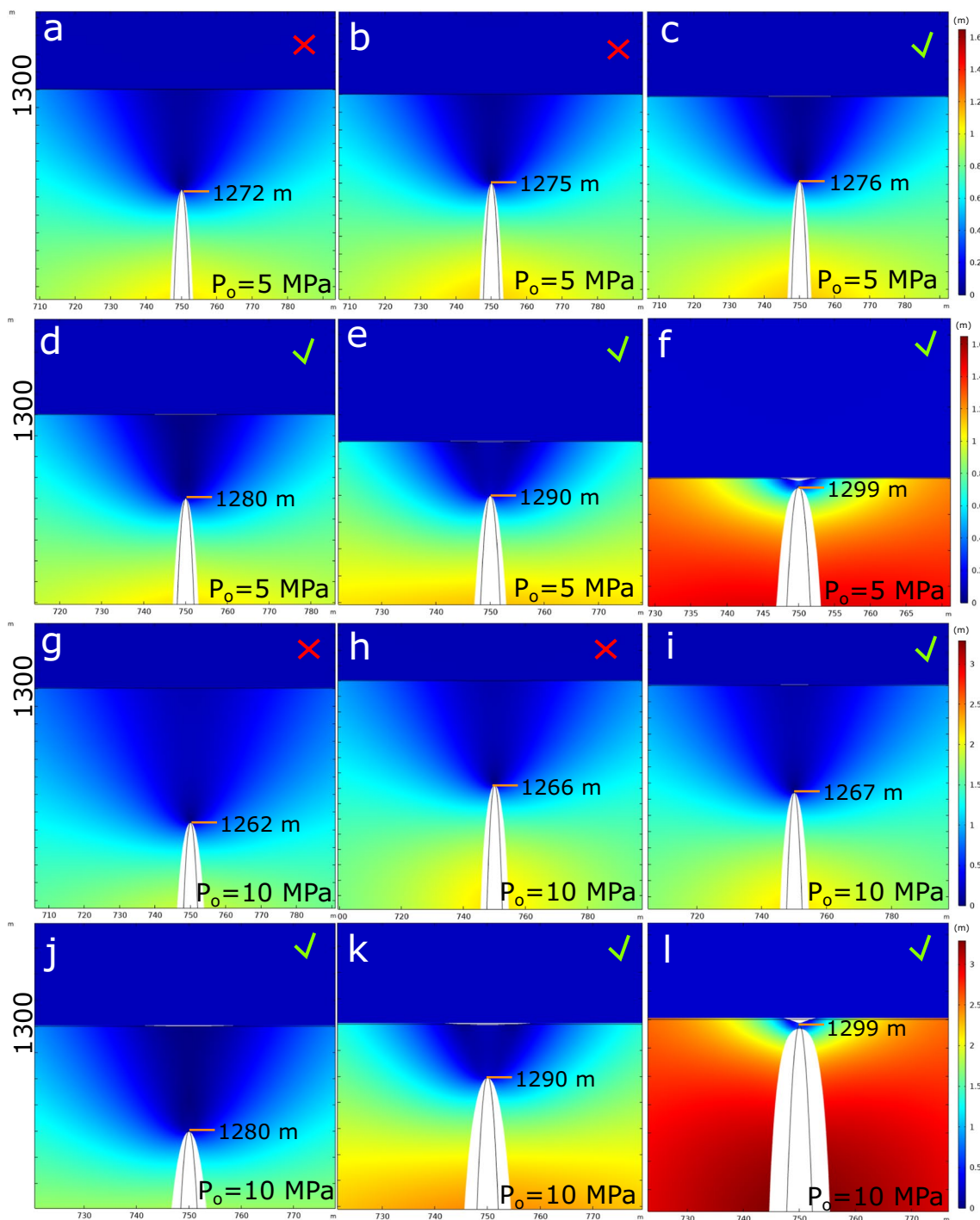


Fig. 5 COMSOL models showing six displacement snapshots (in m) of a dyke in different y - y' locations for 5 MPa (a–f) and 10 MPa (g–l) magmatic overpressure, respectively. The crosses indicate no contact

opening while the ticks indicate opening of the soft contact. The figure snapshots show only a part of the models

tip and the contact. Finally, we reran the models (Fig. 7i, j, k, l) and increased the thickness of the hyaloclastite by two orders of magnitude ($W_h = 100$ m). Our results highlighted that the soft contact opened when the magma overpressure was high regardless of the stiffness of the hyaloclastite.

Especially, when the hyaloclastite was soft the opening was larger. These results suggested that the magma overpressure highly controlled the opening of a mechanically weak contact. Still, the thickness of the soft layer played a fundamental role in the process when the dyke permeated a soft and

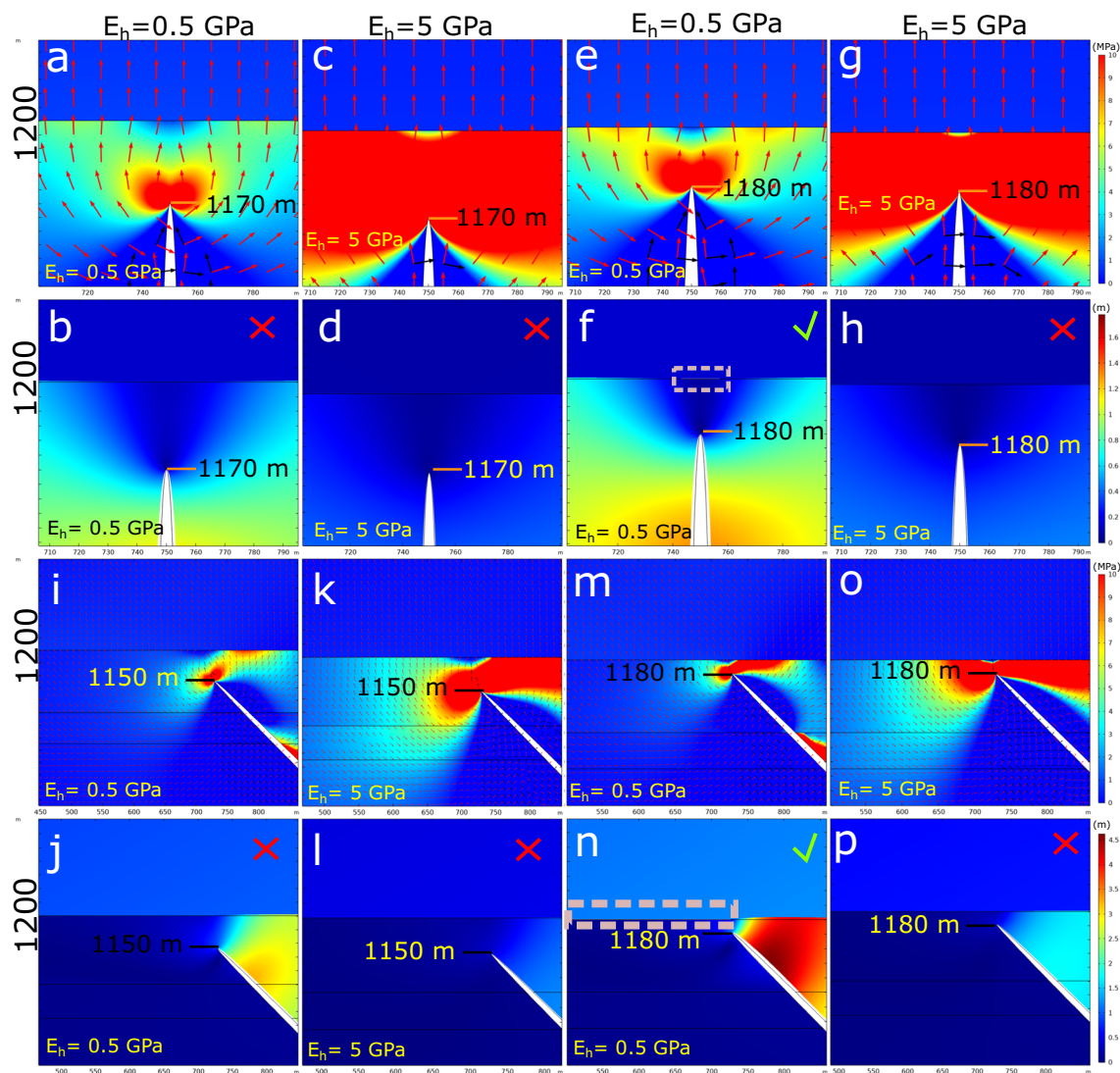


Fig. 6 COMSOL models showing the tensile stress concentration (**a**, **c**, **e**, **g**, **i**, **k**, **m**, **o**) (in MPa) and (x - y) displacement magnitude (**b**, **d**, **f**, **h**, **j**, **l**, **n**, **p**) (in m) around a dyke tip subject to dissimilar host rock mechanical properties (stratigraphy **b**). The magma overpressure is constant ($P_o = 5$ MPa), the red arrows show σ_1 and the black arrows

show σ_2 . The dashed boxes indicate the location and size of the contact opening. The crosses indicate no contact opening while the ticks indicate opening of the soft contact. The figure snapshots show only a part of the models

several meters thick layer. However, when the soft layer was thin, the stiffness of the hyaloclastite controlled the opening of the contact instead.

Glacier retreat due to glacier width adjustments

In this section, we explored how glacier retreat subject to width variations influences the propagation pathway of a dyke in the shallow crust. In the first model suites, we investigated how the stiffness of the hyaloclastite layer, subject to a wide (25 km) and a short (5 km) glacier, promoted (or not) dyke-sill transitions below an ice cap. All models (Fig. 8a–d) showed variable displacement values around the dyke tip

and at its vicinity. In detail, a very wide glacier cap induced higher displacement values in the host rock when the hyaloclastite was soft (Fig. 8a, i); however, contact opening was not encouraged. When the glacier was shorter (5 km), the amount of displacement decreased, and the contact opened when the stiffness of the hyaloclastite was soft (Fig. 8c, g). This is at odds with similar model results in a non-glacial domain (Fig. 8e–h), which showed that the presence of a soft contact encouraged contact opening regardless of the hyaloclastite stiffness. We finally tested the effect of an inclined sheet in the same setting. The results showed that, regardless of the width of the ice cap, contact opening was discouraged in similar depths (Fig. 8i–l), in contrast to non-glacial

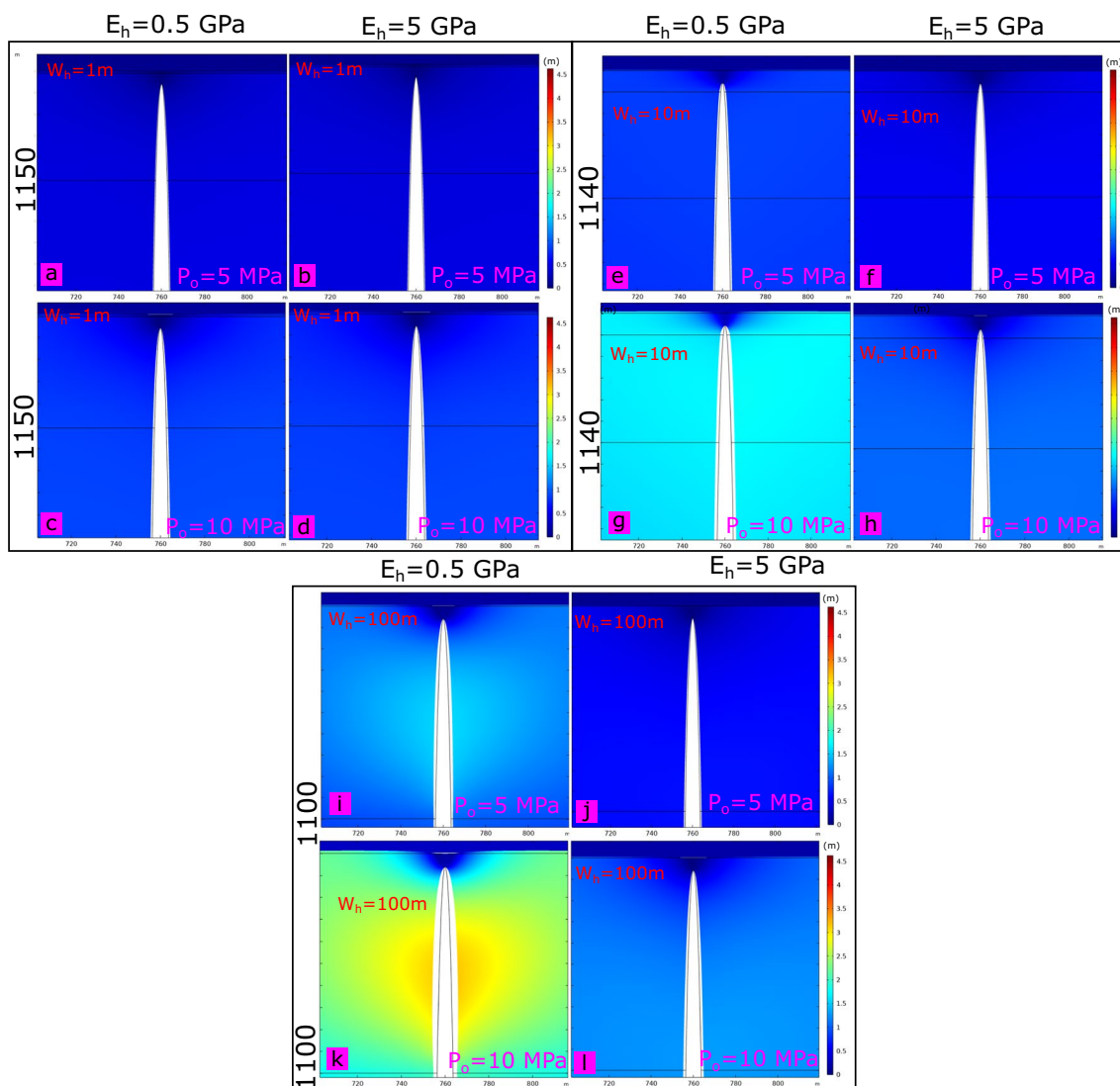


Fig. 7 COMSOL models showing the total (x - y) displacement (in m) around a dyke subject to different values of magma overpressure ($P_o=5$ MPa and $P_o=10$ MPa) and hyaloclastite stiffness ($E_h=0.5$

GPa and $E_h=5$ GPa). The thickness of the hyaloclastite has three different orders of magnitude namely 1 m (a–d), 10 m (e–h) and 100 m (i–l). The figure snapshots show only a part of the models

settings (Fig. 8m–p). Those results indicate that the width of a glacier may affect the dyke-sill transitions in volcanotectonic regimes especially when vertical dykes advance towards the surface. However, the inclined sheet models were insensitive in similar glacier settings (Fig. 8i–l).

Discussion

Which mechanism controlled the emplacement of the Stardalur laccolith?

Although dyke propagation commonly occurs in the shallow crust, dyke-sill transitions are also likely in rift zones. This is mainly due to the heterogeneity and anisotropy of the host

rock that generate stress barriers or dissimilar boundaries (contacts) which either stop or change the pathway of a vertical dyke (Gudmundsson 2020). Those outcomes are controlled by three mechanisms, namely the stress barrier, elastic mismatch and Cook-Gordon debonding and delamination mechanisms, which can act individually or collectively in depth, promoting sill formation (Gudmundsson 2011a).

Our Part II is focused on exploring the mechanical and geometrical parameters that encourage (or not) dyke-sill transitions in non-glacial and glacial domains. To do this, we used a field example, the Stardalur laccolith in SW Iceland, which offered ideal field conditions and the models helped us gain valuable insights into dyke emplacement processes in a more realistic perspective. The laccolith composed of stacked sills and had no signs of dyke rupture at its roof. The

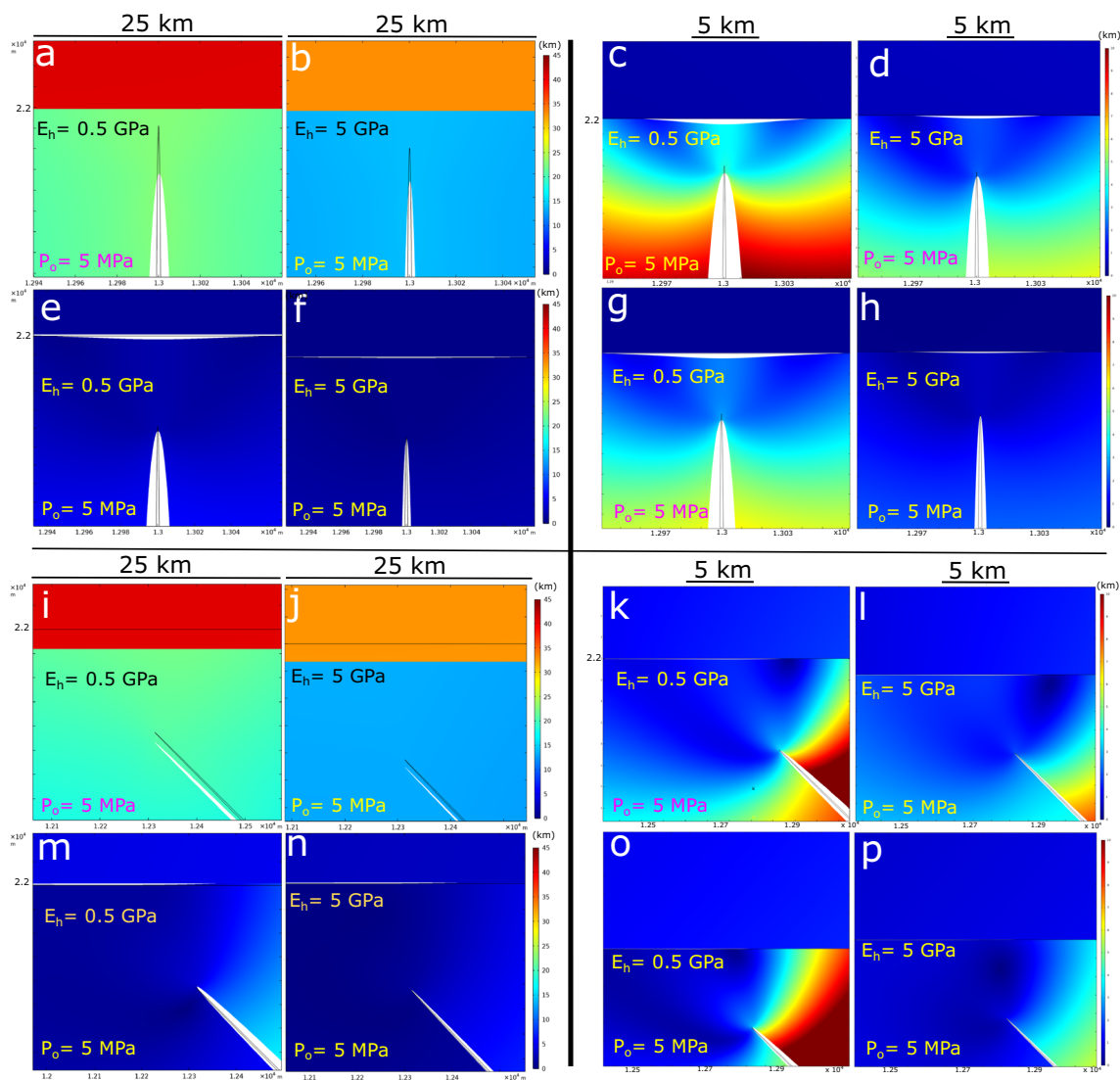


Fig. 8 COMSOL models showing the total (x - y) displacement (in km) around a vertical dyke and an inclined sheet subject to constant overpressure values ($P_o = 5$ MPa), different layer stiffness, in a glacial

(**a-d**, **i-l**) and non-glacial setting (**e-h**, **m-p**). The figure snapshots show only a part of the models

intrusion was emplaced at the contact between two dissimilar layers, namely a lava (top) and a hyaloclastite (bottom) and had an approximate vertical thickness, based on field observations, equal to 150 m.

We suggest that the emplacement of the Stardalur laccolith was primarily induced by the Cook-Gordon debonding and delamination mechanism, though a collective outcome between the elastic mismatch and the Cook-Gordon mechanism cannot be ruled out. This is because the laccolith is very shallow, a case in which the Cook-Gordon mechanism can easily operate (Gudmundsson 2020). The prime boundary loading condition used in our models was the overpressure (P_o) of the dyke. Here, we modelled two values, namely, 5 MPa and 10 MPa to replicate moderate and high magma overpressure conditions, respectively. In

all our models, the tested boundary conditions generated sufficient values of tensile stress ($\sigma_3 \geq 0.5$ MPa) around the dyke/inclined sheet to satisfy the fracture criterion (Amadei and Stephansson 1997). Particularly, high values of magma overpressure encouraged the opening of the mechanically weak contact. This highlights not only the necessity of a thin elastic layer for debonding and delamination to occur (Rosakis et al. 2000; Xu and Rosakis 2003; Wang and Xu 2006), but also how important are the roles of magma overpressure and the mechanical properties of the host rock (especially the layering) on dyke propagation in the shallow crust. Still, those parameters can become secondary in glacial conditions when a dyke propagates below a large ice cap. An ice cap not only overprints the local stress conditions below it (Stewart et al. 2000), but the vertical pressure withholds the

opening of the contact at similar depths since practically the broad stress field becomes compressional (Andrew and Gudmundsson 2007). Nevertheless, our study showed that dyke-sill transitions may equally occur during glacier unloading.

How do different realistic geometrical and mechanical parameters collectively affect the opening of a dissimilar contact in non-glacial and glacial settings?

To allow strict model comparisons between the studied settings, we replicated identical models using the same boundary loading conditions (e.g., overpressure, thin elastic layer boundary load, vertical and horizontal pressure load) by isolating a mechanical or geometrical parameter in each run. Finally, we focused on showing a selected part of each model to allow for a more efficient comparison between different models.

Layer stiffness

The abrupt changes in the mechanical properties of the rocks and especially the Young's modulus (stiffness) may alter the pathways of advancing dykes or inclined sheets in the crust (Gudmundsson 2011a, b, 2020; Kavanagh et al. 2006; Philipp et al. 2013; Drymoni et al. 2020). When a fracture propagates from a soft to a stiff layer, it often becomes arrested or deflected at it. In our models, we explored further than before (Part I, Drymoni et al. 2023c) the effect of the stiffness of a layer in dyke-sill emplacement in non-glacial and glacial settings. We modelled hyaloclastite deposits with Young's moduli over two different orders of magnitude, namely 0.5 GPa and 5 GPa, which implied soft and comparatively stiff mechanical conditions, respectively. In a non-glacial setting, a comparatively stiff hyaloclastite concentrates more tensile stress (σ_3) than a soft one but a soft hyaloclastite promotes dyke-sill transitions compared to a comparatively stiff one. When the layer is very thin (1 m), the opening is greatly controlled by the stiffness of the layer regardless of the depth of the soft contact in the crustal setting. Still, when the overpressure is moderate ($P_o \leq 5$ MPa), dyke-sill transitions can be revoked. Finally, in a glacial setting, a soft hyaloclastite layer concentrates higher amounts of displacement, encourages dyke-sill transitions, and promotes larger contact opening. However, in case the ice cap is wide (25 km), contact opening is discouraged regardless of the stiffness of the hyaloclastite.

Dyke dip

Previous studies have modelled the stresses and displacements around vertical dykes (Drymoni et al. 2020, 2021) and inclined sheets (Gudmundsson and Brenner 2001;

Burchardt 2008; Browning and Gudmundsson 2015; Bazargan and Gudmundsson 2020; Drymoni et al. 2021, 2023a, b, c) in dissimilar mechanical contacts showing that inclined sheets promote higher surface stresses and displacements. Similarly, inclined sheets are more prone to feed sills. Here, we studied the effect of a vertical dyke and an inclined sheet in dyke-sill transitions in non-glacial and glacial settings. The numerical results proposed that inclined sheets tend to open asymmetric sills when the dyke-tip is deeper in the crust compared to vertical dykes. Instead, in glacial settings, inclined sheets discourage contact opening regardless of the width of the ice cap.

Layer thickness

Previous studies (Geshi et al. 2012, Forbes Inskip et al. 2020; Drymoni et al. 2020) have shown that thick, stiff layers (increased by a factor of ten) or layer inclination (Clunes et al. 2021, 2023) can promote stress rotations and arrest dykes or deflect them into sills. We tested the effect of the thickness of a layer in three different orders of magnitude, namely 1 m, 10 m and 100 m, in non-glacial conditions. The results highlighted the importance of this geometrical parameter especially in higher orders of magnitude. When the thickness of the hyaloclastite is hundreds of metres, dyke-sill deflection is always encouraged despite the stiffness of the layer. Still, in lower orders of magnitude (1–10 m), the stiffness of the layer plays a more critical role in contact opening.

Crustal segment /depth of a soft contact

Soft contacts can locally rotate the stress field and produce dyke-sill transitions as shown from experiments (Kavanagh et al. 2017). Yet, the nature of sill propagation is debated between fracture toughness weak boundaries (Menand and Tait 2002) and viscosity dominated processes (Chanceaux and Menand 2016). In our models, we showed that the opening of a contact, hence, the dyke-sill transition, is always dependent to the presence of a soft contact in both non-glacial and glacial settings, an observation that is in agreement with dynamic crack propagation experiments (Rosakis et al. 2000). Here, we modelled two different stratigraphic sequences (stratigraphy a and b) based on our field observations. Our results were inconclusive regarding the effect of the depth of the contact in the stratigraphy in non-glacial settings because the opening of the contact was primarily controlled by the stiffness of the layer. More advanced models should be designed to explore this parameter further.

Dyke tip-contact distance

We designed models to obtain indications on the conditions that affect the opening of a mechanically weak contact ahead of a dyke tip subject to different dyke tip-contact distance and magma overpressure values. Our models imply that higher overpressure values ($P_o \geq 10$ MPa) encourage the opening of the contact when the distance between the dyke and the soft contact is larger.

How do dyke-sill transitions respond to glacial settings with variable glacier widths?

Previous numerical models in Iceland have shown that the large volumes of the lava shields that were generated during the late-glacial (close to the end of the Weischelian) era induced an increased accumulation of tensile stresses around the deep-seated magma chambers. As such they increased their fracture porosity and eventually their sizes (Gudmundsson 1986; Andrew and Gudmundsson 2007). Yet, during the glaciation peaks (e.g. Weischelian era), the glacier-induced compressive regime should have overprinted the crustal local stresses in depth, and only after the deglaciation stage, dyke propagation must have been encouraged (Andrew and Gudmundsson 2007).

In our physics-based modelling study, we test how the width of the ice cap encourages (or not) dyke-sill transitions in the shallow crust. Specifically, our study models the scenario where fractures (vertical dykes or inclined sheets) may stall below an ice cap during glacier retreat. In detail, we attempt to examine the conditions that encourage the mechanical deflection of magma at a more local scale and explore the conditions that promote sill emplacement in heterogeneous domains during deglaciation. Our models show that a vertical dyke may open a soft contact ahead of its tip when the glacier is short (5-km length) and the bottom contact layer is soft. On the contrary, an inclined sheet fails to replicate the previous outcome. This is at odds with the previous theory, which highlights that shorter glaciers in regional scales tend to promote dyke propagation since tensional stresses commonly increase around shallow magma chambers and dyke injection can be prominent (Andrew and Gudmundsson 2007). Our study focuses on dyke to sill deflection in shallow heterogeneous crustal segments and not on the conditions for magma chamber rupture and dyke injection during deglaciation. We also underscore that our static, elastic models attempt to gain insights into processes that occur at the mesoscale and serve as a comparative effort to identify the controlling parameters for dyke-sill transition during glacier retreat. Finally, those processes can have similar effects with modelling the effect of topography exerted by a volcanic edifice. There, analogue (Kervyn et al. 2009), analytical (Maccaferri et al. 2010, 2011) and numerical

(Urbani et al. 2017) studies have shown that the loading stress field alters or stops the propagation pathway of a dyke below an edifice and promotes deflection (or lateral propagation) away from the volcano summit.

Conclusions

Our Part II suggests the following conclusions most of which can have a more general significance:

In non-glacial settings

1. Stiff layers concentrate more tensile stress than soft layers but accommodate less amount of ($x-y$) displacement.
2. Inclined sheets promote contact opening further away from a soft contact compared to vertical dykes. When the tip of the inclined sheet gets gradually shallower, the opening increases laterally opposite to the acute angle of the dip, forming asymmetric sills.
3. Stiff layers tend to discourage sill emplacement regardless of the dyke dip.
4. Dyke-sill transitions occur regardless of the depth of a soft contact.
5. The thickness of a soft layer may encourage dyke-sill transitions. When the magma overpressure is moderate ($P_o = 5$ MPa) and the soft layer is thin, sill emplacement is controlled by the stiffness of the layer. However, when the overpressure of the magma and the thickness of the soft layer both increase, the thickness may encourage the opening of the contact. Hence, very thin layers are not sensitive enough to contact opening.

In glacial settings:

1. The stiffness of the layers, apart from the stress conditions imposed by the ice cap, may also control the opening of a soft contact.
2. Wide ice caps tend to discourage contact opening whereas shorter ice caps may promote sill emplacement under specific conditions.
3. Vertical dykes can form sills easier than inclined sheets.

Recap and final remarks

In Part I, we explored how and under which conditions the Stardalur laccolith in SW Iceland could have been emplaced. We tested different boundary loading conditions to investigate the mechanics of dyke-sill transition in a heterogeneous setting. In non-glacial settings, sills may form due to stiffness contrasts between dissimilar layers in the country rock. Similarly, in compressional regimes implied by pre-existing fractures, stress barriers occur and encourage sill formation.

Finally, during glacier retreat (glacier thinning) and under specific mechanical conditions, dyke to sill deflection can still take place and magma may stall in the shallow crust.

In Part II, we performed several sensitivity analyses to investigate further how close to the contact dyke-sill transitions may happen in non-glacial settings. Our results showed that inclined sheets can open a soft contact further away from it and deeper in the crust than vertical dykes. Meanwhile, higher magma overpressure values encourage the opening of a contact further away from it (deeper in the crust). Furthermore, the stiffness and thickness of the soft layer (hyaloclastite) below the contact are both important factors for dyke-sill transitions. Finally, we examined how dyke-sill transitions respond to glacial settings with variable glacier widths. Comparisons with identical models in non-glacial (volcanotectonic) settings demonstrate that although the conditions for dyke-sill transitions may be satisfied in glacial domains, this is not equally encouraged in volcanotectonic ones and vice versa. Our results suggest that magma storage in the shallow crust could be encouraged during glacier unloading under specific mechanical conditions.

Acknowledgements We thank, the editor Joel Ruch, Steffi Burchardt and John Browning for helpful comments and suggestions as well as Tàrsilo Girona for fruitful discussions. This work was carried out under the aegis of Task Force II of the International Lithosphere Program (Leader A. Tibaldi). K. Drymoni acknowledges a 2-year research fellowship of the Italian Ministry of University and Research in the framework of a Progetto di Eccellenza grant of the Department of Earth and Environmental Sciences of the University of Milan-Bicocca.

Author contribution Conceptualization: Kyriaki Drymoni. Formal analysis and investigation: Kyriaki Drymoni. Visualization: Kyriaki Drymoni. Writing—original draft preparation: Kyriaki Drymoni. Conceptualization of field data: Alessandro Tibaldi and Federico Pasquare Mariotto. Review and editing: Kyriaki Drymoni, Alessandro Tibaldi, Federico Pasquare Mariotto, and Fabio Luca Bonali.

Funding Open access funding provided by Università degli Studi di Milano - Bicocca within the CRUI-CARE Agreement.

Open Access This article is licensed under a Creative Commons Attribution 4.0 International License, which permits use, sharing, adaptation, distribution and reproduction in any medium or format, as long as you give appropriate credit to the original author(s) and the source, provide a link to the Creative Commons licence, and indicate if changes were made. The images or other third party material in this article are included in the article's Creative Commons licence, unless indicated otherwise in a credit line to the material. If material is not included in the article's Creative Commons licence and your intended use is not permitted by statutory regulation or exceeds the permitted use, you will need to obtain permission directly from the copyright holder. To view a copy of this licence, visit <http://creativecommons.org/licenses/by/4.0/>.

References

- Acocella V (2000) Space accommodation by roof lifting during pluton emplacement at Amiata (Italy). *Terra Nova* 12:149–155
- Acocella V (2021) *Volcano-tectonic processes*, vol 567. Springer, Switzerland
- Ahn BK, Curtin WA, Parthasarathy TA, Dutton RE (1998) Criterion for crack deflection/penetration for fiber-reinforced ceramic matrix composites. *Compos Sci Technol* 58:1775–1784
- Amadei B, Stephansson O (1997) *Rock stress and its measurement*. Springer Science & Business Media, Dordrecht
- Anderson EM (1951) *Dynamics of faulting and dyke formation*, 2nd edn. Olivier and Boyd, Edinburgh
- Andrew RE, Gudmundsson A (2007) Distribution, structure, and formation of Holocene lava shields in Iceland. *J Volcanol Geoth Res* 168:137–154
- Annen C (2009) From plutons to magma chambers: thermal constraints on the accumulation of eruptible silicic magma in the upper crust. *Earth Planet Sci Lett* 284(3–4):409–416
- Annen C, Blundy JD, Sparks RSJ (2006) The genesis of intermediate and silicic magmas in deep crustal hot zones. *J Petr* 47:505–539
- Árnadóttir S, Thordarson T, Hjartarson Á, Gautason B (2023) U-Pb zircon age and chronology of the Torfufell central volcano: implications for timing of rift relocation in North Iceland. *Bull Volcanol* 85:52
- Barber AH, Wiesel E, Wagner HD (2002) Crack deflection at a transcrystalline junction. *Compos Sci Technol* 62:1957–1964
- Barnett ZA, Gudmundsson A (2014) Numerical modelling of dykes deflected into sills to form a magma chamber. *J Volcanol Geoth Res* 281:1–11
- Bazargan M, Gudmundsson A (2020) Stresses and displacements in layered rocks induced by inclined (cone) sheets. *J Volcanol Geoth Res* 401:106965
- Björnsson H, Gudmundsson S, Jóhannesson T, Pálsson F, Aðalgeirsdóttir G, Haraldsson HH (2006) Geometry, mass balance and climate change response of Langjökull ice cap, Iceland. The International Arctic Science Committee (IASC), Working Group on Arctic Glaciology
- Browning J, Gudmundsson A (2015) Caldera faults capture and deflect inclined sheets: an alternative mechanism of ring dike formation. *Bull Volcanol* 77:1–13
- Browning J, Karaoğlu Ö, Bayer Ö, Turgay MB, Acocella V (2021) Stress fields around magma chambers influenced by elastic thermo-mechanical deformation: implications for forecasting chamber failure. *Bull Volcanol* 83:1–13
- Bunger AP, Cruden AR (2011) Modelling the growth of laccoliths and large mafic sills: role of magma body forces. *J Geophys Res* 116:B02203. <https://doi.org/10.1029/2010JB007648>
- Burchardt S (2008) New insights into the mechanics of sill emplacement provided by field observations of the Njardvik Sill, North-east Iceland. *J Volcanol Geoth Res* 173:280–288
- Cashman KV, Sparks RSJ, Blundy JD (2017) Vertically extensive and unstable magmatic systems: a unified view of igneous processes. *Science* 355(6331):eaag3055
- Chanceaux L, Menand T (2016) The effects of solidification on sill propagation dynamics and morphology. *Earth Planet Sci Lett* 442:39–50
- Clunes M, Browning J, Cembrano J, Marquardt C, Gudmundsson A (2021) Crustal folds alter local stress fields as demonstrated by magma sheet—fold interactions in the Central Andes. *Earth Planet Sci Lett* 570:117080
- Clunes M, Browning J, Marquardt C, Cortez J, Drymoni K, Kavanagh J (2023) Inclination and heterogeneity of layered geological sequences influence dike-induced ground deformation. *Geology* 51:278–283
- Coleman DS, Gray W, Glazner AF (2004) Rethinking the emplacement and evolution of zoned plutons: geochronologic evidence for incremental assembly of the Tuolumne Intrusive Suite. *Calif Geol* 32:433–436

- Cook J, Gordon JE (1964) A Mechanism for the Control of Crack Propagation in All-Brittle Systems. *Proc R Soc* 282:1364–5021. <https://doi.org/10.1098/rspa.1964.0248>
- Corry CE (1988) *Laccoliths: mechanics of emplacement and growth* (vol 220). Geological Society of America
- Corti N, Bonali FL, Russo E, Drymoni K, Mariotto FP, Gudmundsson A, Esposito R, Cavallo A, Tibaldi A (2023) Feeders vs arrested dikes: a case study from the Younger Stampar eruption in Iceland. *J Volcanol Geotherm Res* 443:107914
- Cruden AR (1998) On the emplacement of tabular granites. *J Geol Soc* 155(5):853–862
- Cruden AR, McCaffrey KJ (2001) Growth of plutons by floor subsidence: implications for rates of emplacement, intrusion spacing and melt-extraction mechanisms. *Phys Chem Earth Part A* 26:303–315
- Cruden AR, Weinberg RF (2018) Mechanisms of magma transport and storage in the lower and middle crust—magma segregation, ascent and emplacement. *Volcanic Igneous Plumbing Syst* 13–53
- Depree N, Sneyd J, Taylor S, Taylor MP, Chen JJ, Wang S, O'Connor M (2010) Development and validation of models for annealing furnace control from heat transfer fundamentals. *Comput Chem Eng* 34:1849–1853
- Drymoni K (2020) Dyke propagation paths: the movement of magma from the source to the surface. PhD thesis. University of London, UK
- Drymoni K, Browning J, Gudmundsson A (2020) Dyke-arrest scenarios in extensional regimes: insights from field observations and numerical models, Santorini, Greece. *J Volcanol Geoth Res* 396:106854
- Drymoni K, Browning J, Gudmundsson A (2021) Volcanotectonic interactions between inclined sheets, dykes, and faults at the Santorini Volcano, Greece. *J Volcanol Geoth Res* 416:107294
- Drymoni K, Browning J, Gudmundsson A (2022) Spatial and temporal volcanotectonic evolution of Santorini volcano Greece. *Bull Volcanol* 84:60
- Drymoni K, Russo E, Tibaldi A, Corti N, Bonali FL, Mariotto FP (2023a) Dyke-induced graben formation in a heterogeneous succession on Mt. Etna: insights from field observations and FEM numerical models. *J Volcanol Geotherm Res* 433:107712
- Drymoni K, Browning J, Pomonis P, Magganis A (2023b) Historical accounts provide insight on the geological evolution of the 20th century eruptions at Santorini volcano Greece. *Bull Volcanol* 85:70
- Drymoni K, Tibaldi A, Bonali FL, Mariotto FAP (2023c) Dyke to sill deflection in the shallow heterogeneous crust during glacier retreat: part I. *Bull Volcanol* 85:73
- Dundurs J (1969) Edge-bonded dissimilar orthogonal wedges. *J Appl Mech* 36:650–652
- Evans AG, Zok FW (1994) Review the physics and mechanics of fiber-reinforced brittle matrix composites. *J Mater Sci* 29:3857–3896
- Fedotov SA (1981) Magma rates in feeding conduits of different volcanic centers. *J Volc Geoth Res* 9:379–394
- Fialko YA, Khazan Y, Simons M (2001) Deformation due to a pressurized horizontal circular crack in an elastic half-space, with application to volcano geodesy. *Geophys Int J* 146:181–190
- Forbes Inskip ND, Browning J, Meredith PG, Gudmundsson A (2020) Conditions for fracture arrest in layered rock sequences. *Results Geophys Sci* 1:100001
- Forslund T, Gudmundsson A (1991) Crustal spreading due to dikes and faults in southwest Iceland. *J Struct Geol* 13:443–457
- Francis EH (1982) Magma and sediment-I Emplacement mechanism of late Carboniferous tholeiite sills in northern Britain: President's anniversary address 1981. *J Geol Soc* 139(1):1–20
- Freund LB, Suresh S (2003) *Thin Film Materials: Stress, Defect Formation and Surface Evolution*. Cambridge University Press, Cambridge
- Fridleifsson IB (1977) Distribution of large basaltic intrusions in the Icelandic crust and the nature of the layer 2–layer 3 boundary. *Geol Soc Am Bull* 88:1689–1693
- Galerne CY, Neumann ER, Planke S (2008) Emplacement mechanisms of sill complexes: information from the geochemical architecture of the Golden Valley Sill Complex, South Africa. *J Volcanol Geoth Res* 177:425–440
- Galland O, Planke S, Neumann E-R, Malthe-Sørensen A (2009) Experimental modelling of shallow magma emplacement: application to saucer-shaped intrusions. *Earth Planet Sci Lett* 277:373–383. <https://doi.org/10.1016/j.epsl.2008.11.003>
- Galland O, Bertelsen HS, Eide CH, Guldstrand F, Haug ØT, Leanza HA, ... Spacapan JB (2018) Storage and transport of magma in the layered crust—formation of sills and related flat-lying intrusions. In: *Volcanic and igneous plumbing systems*. Elsevier. <https://doi.org/10.1016/B978-0-12-809749-6.00005-4>
- Galland O, Spacapan JB, Rabbel O, Mair K, Soto FG, Eiken T, ... Leanza HA (2019) Structure, emplacement mechanism and magma-flow significance of igneous fingers—Implications for sill emplacement in sedimentary basins. *J Struct Geol* 124:120–135
- García IG (2014) Crack initiation in composites at micro and meso scales: development and applications of finite fracture mechanics (Doctoral dissertation, Universidad de Sevilla)
- Gautneb H, Gudmundsson A, Oskarsson N (1989) Structure, petrochemistry and evolution of a sheet swarm in an Icelandic central volcano. *Geol Mag* 126:659–673
- Geshi N, Kusumoto S, Gudmundsson A (2012) Effects of mechanical layering of host rocks on dike growth and arrest. *J Volcanol Geoth Res* 223:74–82
- Gilbert GK (1877) Report on the geology of the Henry Mountains. U.S. Geogr. Geol. Surv. Rocky Mountain Region (Powel), p. 160
- Glazner AF, Bartley JM, Coleman DS, Gray W, Taylor RZ (2004) Are plutons assembled over millions of years by amalgamation from small magma chambers? *GSA today* 14(5-Apr):4–11
- Gordon JE (1976) *The new science of strong materials*, 2nd edn. Pitman Publishing Limited, London
- Gori M, Rubino V, Rosakis AJ, Lapusta N (2018) Pressure shock fronts formed by ultra-fast shear cracks in viscoelastic materials. *Nat Commun* 9:4754
- Greiner SH, Burchardt S, Sigmundsson F, Óskarsson BV, Galland O, Geirsson H, Rhodes E (2023) Interaction between propagating basaltic dikes and pre-existing fractures: a case study in hyaloclastite from Dyrhöfjöll, Iceland. *J Volcanol Geoth Res* 442:107891
- Gressier JB, Mourgues R, Bodet L, Matthieu JY, Galland O, Cobbold P (2010) Control of pore fluid pressure on depth of emplacement of magmatic sills: an experimental approach. *Tectonophysics* 489:1–13
- Gretener PE (1969) On the mechanics of the intrusion of sills. *Can J Earth Sci* 6:1415–1419
- Grosfils EB, McGovern PJ, Gregg PM, Galgana GA, Hurwitz DM, Long SM, Chestler SR (2015) Elastic models of magma reservoir mechanics: a key tool for investigating planetary volcanism. *Geol Soc London, Special Publ* 401:239–267
- Gudmundsson A (1986) Mechanical aspects of postglacial volcanism and tectonics of the Reykjanes Peninsula, southwest Iceland. *J Geophys Res: Solid Earth* 91:12711–12721
- Gudmundsson A (1990) Emplacement of dikes, sills and crustal magma chambers at divergent plate boundaries. *Tectonophysics* 176:257–275
- Gudmundsson A (1995) Infrastructure and mechanics of volcanic systems in Iceland. *J Volcanol Geoth Res* 64:1–22
- Gudmundsson A (2003) Surface stresses associated with arrested dykes in rift zones. *Bull Volcanol* 65:606–619
- Gudmundsson A (2011a) *Rock fractures in geological processes*. Cambridge University Press, Cambridge

- Gudmundsson A (2011b) Deflection of dykes into sills at discontinuities and magma-chamber formation. *Tectonophysics* 500:50–64
- Gudmundsson A (2012) Magma chambers: formation, local stresses, excess pressures, and compartments. *J Volcanol Geoth Res* 237:19–41
- Gudmundsson A (2020) *Volcanotectonics: understanding the structure, deformation and dynamics of volcanoes*. Cambridge University Press, Cambridge
- Gudmundsson A, Brenner SL (2001) How hydrofractures become arrested. *Terra Nova* 13:456–462
- Gudmundsson A, Løtveit IF (2012) Sills as fractured hydrocarbon reservoirs: examples and models *Geol Soc Lond Spec Publ* 374. <https://doi.org/10.1144/SP374.5>
- Gudmundsson A, Pasquarè FA, Tibaldi A (2018) Dykes, sills, laccoliths, and inclined sheets in Iceland. *Physical Geology of Shallow Magmatic Systems: Dykes, Sills and Laccoliths*, pp 363–376
- Gupta V, Argon AS, Suo Z (1992) Crack deflection at an interface between two orthotropic media. *ASME J Appl Mech* 59(2S):S79–S87
- Hansen DM, Cartwright J (2006) Saucer-shaped sill with lobate morphology revealed by 3D seismic data: implications for resolving a shallow-level sill emplacement mechanism. *J Geol Soc* 163:509–523
- Hansen DM, Cartwright JA, Thomas D (2004) 3D seismic analysis of the geometry of igneous sills and sill junction relationships. *Geol Soc, London, Memoirs* 29:199–208
- Hardee HC (1982) Incipient magma chamber formation as a result of repetitive intrusions. *Bull Volcanol* 45:41–49
- Haug OT, Galland O, Souloumiac P, Souche A, Guldstrand F, Schmiedel T et al (2018) Shear versus tensile failure mechanisms induced by sill intrusions—implications for emplacement of conical and saucer-shaped intrusions. *J Geophys Res* 123:1–20. <https://doi.org/10.1002/2017JB015196>
- He MY, Evans AG, Hutchinson JW (1994) Crack deflection at an interface between dissimilar elastic materials: role of residual stresses. *Int J Solids Struct* 31:3443–3455
- He MY, Hutchinson JW (1989) Kinking of a crack out of an interface. *J Appl Mech* 56:270–278
- Hutchinson JW, Suo Z (1992) Mixed Mode Cracking in Layered Materials. *Adv Appl Mech* 29:63–191
- Jaeger JC (1959) Temperatures outside a Cooling Intrusive Sheet. *Science* 257:44–54
- Kavanagh JL, Menand T, Sparks RSJ (2006) An experimental investigation of sill formation and propagation in layered elastic media. *Earth Planet Sci Lett* 245:799–813
- Kavanagh JL, Boutelier D, Cruden AR (2015) The mechanics of sill inception, propagation and growth: experimental evidence for rapid reduction in magmatic overpressure. *Earth Planet Sci Lett* 421:117–128
- Kavanagh JL, Rogers BD, Boutelier D, Cruden AR (2017) Controls on sill and dyke-sill hybrid geometry and propagation in the crust: the role of fracture toughness. *Tectonophysics* 698:109–120
- Kavanagh JL, Burns AJ, Hazim SH, Wood EP, Martin SA, Hignett S, Dennis DJ (2018) Challenging dyke ascent models using novel laboratory experiments: implications for reinterpreting evidence of magma ascent and volcanism. *J Volcanol Geoth Res* 354:87–101
- Kervyn M, Ernst GGJ, van Wyk de Vries B, Mathieu L, Jacobs P (2009) Volcano load control on dyke propagation and vent distribution: insights from analogue modeling. *J Geophys Res: Solid Earth* 114(B3)
- Kim JW, Bhowmick S, Hermann I, Lawn BR (2006) Transverse fracture of brittle bilayers: relevance to failure of all-ceramic dental crowns. *J Biomed Mater Res* 79B:58–65
- Kusumoto S, Geshi N, Gudmundsson A (2013) Aspect ratios and magma overpressures of non-feeder dikes observed in the Miyake-jima volcano (Japan), and fracture toughness of its upper part. *Geophys Res Lett* 40(1–5). <https://doi.org/10.1002/grl.50284>
- Lee W, Howard SJ, Clegg WJ (1996) Growth of interface defects and its effect on crack deflection and toughening criteria. *Acta Mater* 44(10):3905–3922
- Lee W, Yoo YH, Shin H (2004) Reconsideration of crack deflection at planar interfaces in layered systems. *Compos Sci Technol* 64:2415–2423
- Leguillon D, Lacroix C, Martin E (2001) Crack deflection by an interface—asymptotic of the residual thermal stresses. *Int J Solids Struct* 38:7423–7445
- Maccaferri F, Bonafede M, Rivalta E (2010) A numerical model of dyke propagation in layered elastic media. *Geophys J Int* 180:1107–1123
- Maccaferri F, Bonafede M, Rivalta E (2011) A quantitative study of the mechanisms governing dike propagation, dike arrest and sill formation. *J Volcanol Geoth Res* 208(1–2):39–50
- Macdonald KC (1982) Mid-ocean ridges: fine scale tectonic, volcanic and hydrothermal processes within the plate boundary zone. *Annu Rev Earth Planet Sci* 10:155–190
- Magee C, Jackson CAL, Schofield N (2013) The influence of normal fault geometry on igneous sill emplacement and morphology. *Geology* 41:407–410
- Magee C, Bastow ID, de Vries BVW, Jackson CAL, Hetherington R, Hagos M, Hoggett M (2017) Structure and dynamics of surface uplift induced by incremental sill emplacement. *Geology* 45:431–434
- Magee C, Muirhead JD, Karvelas A, Holford SP, Jackson CA, Bastow ID, ... Shtukert O (2016) Lateral magma flow in mafic sill complexes. *Geosphere* 12:809–841
- Majumdar BS, Gundel DB, Dutton RE, Warriar SG, Pagano NJ (1998) Evaluation of the tensile interface strength in brittle matrix composite systems. *J Am Ceram Soc* 81:1600–1610
- Martinez D, Gupta V (1994) Energy criterion for crack deflection at an interface between two orthotropic media. *J Mech Phys Solids* 42:1247–1271
- Mathieu L, Burchardt S, Troll VR, Krumbholz M, Delcamp A (2015) Geological constraints on the dynamic emplacement of cone-sheets—the Ardnamurchan cone-sheet swarm, NW Scotland. *J Struct Geol* 80:133–141
- Menand T (2008) The mechanics and dynamics of sills in layered elastic rocks and their implications for the growth of laccoliths and other igneous complexes. *Earth Sci Planet Lett* 267:93–99
- Menand T, Tait SR (2002) The propagation of a buoyant liquid-filled fissure from a source under constant pressure: an experimental approach. *J Geophys Res: Solid Earth* 107(B11):ECV-16
- Menand T, Daniels KA, Benghiat P (2010) Dyke propagation and sill formation in a compressive tectonic environment. *J Geophys Res: Solid Earth* 115:B8
- Merle O, Donnadieu F (2000) Indentation of volcanic edifices by the ascending magma. *Geol Soc Lond Spec Publ* 174:43–53
- Michel J, Baumgartner L, Putlitz B, Schaltegger U, Ovtcharova M (2008) Incremental growth of the Patagonian Torres del Paine laccolith over 90 ky. *Geology* 36(6):459–462
- Morgan S (2018) Pascal’s principle, a simple model to explain the emplacement of laccoliths and some mid-crustal plutons. In: *Volcanic and igneous plumbing systems*. Elsevier, pp 139–165
- Morgan S, Stanik A, Horsman E, Tikoff B, de Saint Blanquat M, Habert G (2008) Emplacement of multiple magma sheets and wall rock deformation: Trachyte Mesa intrusion, Henry Mountains Utah. *J Struct Geol* 30:491–512
- Parsons T, Sleep NH, Thompson GA (1992) Host rock rheology controls on the emplacement of tabular intrusions: implications for underplating of extended crust. *Tectonics* 11:1348–1356
- Pasquarè FA, Tibaldi A (2007) Structure of a sheet-laccolith system revealing the interplay between tectonic and magma stresses

- at Stardalur Volcano Iceland. *J Volcanol Geotherm Res* 161:131–150
- Pedicini M, Bonali FL, Corti N, Mariotto FP, Drymoni K, Tibaldi A (2023) A step forward to understanding the development of volcanotectonic rifts: structure of the Fremrinamar Fissure Swarm (Iceland). *Front Earth Sci* 11:1271721
- Petford N, Cruden AR, McCaffrey KJWV, J.L., (2000) Granite magma formation, transport and emplacement in the Earth's crust. *Nature* 408:669–673
- Petraske KA, Dennis SH, Shaw R (1978) Mechanics of emplacement of basic intrusions. *Tectonophysics* 46:41
- Philipp SL, Afşar F, Gudmundsson A (2013) Effects of mechanical layering on hydrofracture emplacement and fluid transport in reservoirs. *Front Earth Sci* 1:4
- Pinel V, Jaupart C (2000) The effect of edifice load on magma ascent beneath a volcano. *Philos Trans R Soc London A* 358:1515–1532
- Pinel C, Jaupart C (2004) Magma storage and horizontal dyke injection beneath a volcanic edifice *Earth Planet. Sci Lett.* 221:245–262
- Pollard DD (1973) Derivation and evaluation of a mechanical model for sheet intrusions. *Tectonophysics* 19:233–269
- Pollard DD, Holzhausen G (1979) On the mechanical interaction between a fluid-filled fracture and the Earth's surface. *Tectonophysics* 53:27–57
- Pollard DD, Johnson AM (1973) Mechanics of growth of some laccolithic intrusions in the Henry Mountains, Utah II: bending and failure of overburden and sill formation. *Tectonophysics* 18:311–354
- Pollard DD (1987) Theoretical displacements and stresses near fractures in rock: with applications to faults, joints, veins, dikes, and solution surfaces. *Fracture mechanics of rock*, pp 277–349
- Rivalta E, Böttlinger M, Dahm T (2005) Buoyancy-driven fracture ascent: experiments in layered gelatine. *J Volcanol Geoth Res* 144:273–285
- Roberts JL (1971) On the mechanics of the intrusion of sills: discussion. *Can J Earth Sci* 8:176–179
- Roham S, Hardikar K, Woytowicz P (2004) Crack penetration and deflection at a bimaterial interface in a four-point bend test. *J Mater Res* 19:3019–3027
- Roman DC, Moran SC, Power JA, Cashman KV (2004) Temporal and spatial variation of local stress fields before and after the 1992 eruptions of Crater Peak vent, Mount Spurr volcano, Alaska. *Bull Seismol Soc Am* 94:2366–2379
- Rosakis AJ (2002) Intersonic shear cracks and fault ruptures. *Adv Phys* 51:1189–1257
- Rosakis AJ, Samudrala O, Singh RP, Shukla A (1998) Intersonic crack propagation in bimaterial systems. *J Mech Phys Solids* 46:1789–1814
- Rosakis AJ, Samudrala O, Coker D (2000) Intersonic shear crack growth along weak planes *Mater Res. Innovations* 3:236–243
- Rubin AM (1993) Tensile fracture of rock at high confining pressure: implications for dike propagation. *J Geophys Res: Solid Earth* 98:15919–15935
- Rubin AM (1995) Propagation of magma filled cracks. *Ann Rev Earth Planet Sci* 23:287–336. <https://doi.org/10.1146/annurev.ea.23.050195.001443>
- Schmiedel T, Galland O, Breitzkreuz C (2017) Dynamics of sill and laccolith emplacement in the brittle crust: role of host rock strength and deformation mode. *J Geophys Res: Solid Earth* 122:8860–8871
- Schofield NJ, Brown DJ, Magee C, Stevenson CT (2012) Sill morphology and comparison of brittle and non-brittle emplacement mechanisms. *J Geol Soc* 169:127–141
- Shull KR (2002) Contact mechanics and the adhesion of soft solids. *Mater Sci Eng R Rep* 36:1–45
- Smallwood JR, Maresh J (2002) The properties, morphology and distribution of igneous sills. In: Jolley DW, Bell BR (eds) *The north Atlantic igneous province: stratigraphy, tectonic, volcanic and magmatic processes.* *Geol Soc Lond Spec Publ* 197:271–306
- Smith RL, Shaw HR (1975) Igneous-related geothermal systems. In: White DE, Williams DL (eds) *Assessment of geothermal resources of the United States*, USGS circular 726:58–83
- Srinivasan DV, Idapalapati S (2021) Review of debonding techniques in adhesively bonded composite structures for sustainability. *Sustain Mater Technol* 30:e00345
- Stephens TL, Walker RJ, Healy D, Bubeck A, England RW (2018) Mechanical models to estimate the paleostress state from igneous intrusions. *Solid Earth* 9:847–858
- Stewart IS, Sauber J, Rose J (2000) Glacio-seismotectonics: ice sheets, crustal deformation and seismicity *Quat. Sci Rev* 19:1367–1389
- Sun CT, Jin ZH (2012) *Fracture mechanics.* Academic Press
- Thomson K (2007) Determining magma flow in sills, dykes and laccoliths and their implications for sill emplacement mechanisms. *Bull Volcanol* 70:183–201
- Thomson K, Hutton D (2004) Geometry and growth of sill complexes: insights using 3D seismic from the North Rockall Trough. *Bull Volcanol* 66:364–375
- Thomson K, Schofield N (2008) Lithological and structural controls on the emplacement and morphology of sills in sedimentary basins. *Geol Soc London Spec Publ* 302:31–44
- Tibaldi A (2015) Structure of volcano plumbing systems: a review of multi-parametric effects. *J Volcanol Geoth Res* 298:85–135
- Tibaldi A, Pasquaré MF (2008) A new mode of inner volcano growth: the “flower intrusive structure.” *Earth Planet Sci Lett* 271:202–208
- Tibaldi A, Vezzoli L, Pasquaré FA, Rust D (2008) Strike-slip fault tectonics and the emplacement of sheet-laccolith systems: the Thverfell case study (SW Iceland). *J Struct Geol* 30:274–290
- Tibaldi A, Bonali FL, Corti N, Russo E, Drymoni K, De Beni E, Branca S, Neri M, Cantarero M, Pasquaré Mariotto F (2022) Surface deformation during the 1928 fissure eruption of Mt. Etna (Italy): insights from field data and FEM numerical modelling. *Tectonophysics* 837:229468
- Urbani S, Acocella V, Rivalta E, Corbi F (2017) Propagation and arrest of dikes under topography: models applied to the 2014 Bardarbunga (Iceland) rifting event. *Geophys Res Lett* 44:6692–6701
- Valentine GA, Krogh KE (2006) Emplacement of shallow dikes and sills beneath a small basaltic volcanic center—the role of pre-existing structure (Paiute Ridge, southern Nevada, USA). *Earth Planet Sci Lett* 246:217–230
- Walker RJ, Healy D, Kawanzaruwa TM, Wright KA, England RW, McCaffrey KJW, ... Blenkinsop TG (2017) Igneous sills as a record of horizontal shortening: the San Rafael subvolcanic field, Utah. *Bulletin* 129:1052–1070
- Walker RJ, Gill SPA (2020) Tectonic stress controls saucer-shaped sill geometry and emplacement mechanism. *Geology* 48:898–902
- Wang LP, Xu R (2006) Dynamic interfacial debonding initiation induced by an incident crack. *Int J Solids Struct* 43:6535–65507-391
- Watanabe T, Koyaguchi T, Seno T (1999) Tectonic stress controls on ascent and emplacement of magmas. *J Volcanol Geotherm Res* 91:65–78
- Xu R, Huang YY, Rosakis AJ (2003) Dynamic crack deflection and penetration at interfaces in homogeneous materials: experimental studies and model predictions. *J Mech Phys Solids* 51:461–486
- Xu R, Rosakis AJ (2003) An experimental study of impact-induced failure events in homogeneous layered materials using dynamic photoelasticity and high-speed photography. *Optics Lasers Eng* 40(4):263–288